Geomorphology 445 (2024) 108994

Contents lists available at ScienceDirect

Geomorphology

journal homepage: www.journals.elsevier.com/geomorphology

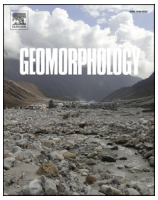

Pleistocene valley incision, landscape evolution and inferred tectonic uplift in the central parts of the Balkan Peninsula – Insights from the geochronology of cave deposits in the lower part of Crna Reka basin (N. Macedonia)

Marjan Temovski [a,b,c,*], Alexander Wieser [d], Oscar Marchhart [d], Mihály Braun [a], Balázs Madarász [e], Gabriella Ilona Kiss [a], László Palcsu [a], Zsófia Ruszkiczay-Rüdiger [b,c]

[a] Isotope Climatology and Environmental Research Centre, HUN-REN Institute for Nuclear Research (ATOMKI), Bem tér 18/c, 4026 Debrecen, Hungary
[b] Institute for Geological and Geochemical Research, HUN-REN Research Centre for Astronomy and Earth Sciences, Budaörsi út 45, 1112 Budapest, Hungary
[c] CSFK, MTA Centre of Excellence, Konkoly Thege Miklós út 15-17., 1121 Budapest, Hungary
[d] University of Vienna, Faculty of Physics - Isotope Physics, Austria, Waehringer Strasse 17, 1090 Wien, Austria
[e] Geographical Institute, HUN-REN Research Centre for Astronomy and Earth Sciences, Budaörsi út 45, 1112 Budapest, Hungary

ARTICLE INFO

Keywords:
Karst
Cave deposits
U-Th dating
Cosmogenic nuclides burial dating

ABSTRACT

Although the general geomorphology is reasonably well understood, not much information is available on the incision rates of rivers and related tectonic uplift in the central parts of the Balkan Peninsula. Caves in the lower part of Crna Reka drainage (N. Macedonia) provide the possibility to reconstruct the Neogene-Quaternary evolution of this area, as previous research has identified two major cave development phases: one related to Pliocene-Early Pleistocene basin infilling and establishment of lacustrine environments, and a subsequent cave development phase related to valley incision due to draining of the lacustrine systems and tectonic uplift.

Here, we present new geochronological data obtained by U-Th dating on speleothems and cosmogenic nuclide burial age determination of clastic cave sediments, that provide time constraints on the Pleistocene karst and valley evolution, and an insight into the related tectonic uplift. The obtained cosmogenic nuclide burial age (2.1 ± 0.5 Ma) of the clastic cave sediments from Temna Peštera – Dragožel, further supports previous results on placing the onset of the draining of the Pliocene lakes in Macedonia in the Early Pleistocene. The similar timing obtained for the downstream and upstream parts of Crna Reka drainage suggests that the draining was more likely initiated by regional uplift, rather than headward erosion related to subsidence in the Aegean Sea. The Middle to Late Pleistocene age of the dated speleothems agrees well with the existing conceptual model for karst and landscape evolution in the area. The cumulative valley incision rates based on these radiometric data show an increase towards the present, with values of <0.1 m/ka in Early Pleistocene, increasing to ~0.2–0.5 m/ka in Middle Pleistocene, and up to 1 m/ka in Late Pleistocene. They are lower than the measured uplift rates in the area (1.1–1.2 m/ka), and mostly overlap with the range of GPS-based vertical deformation rates in the Hellenides. Higher Middle to Late Pleistocene uplift rate is inferred in the downstream part of Crna Reka, an area in the Vardar zone bounded by seismogenic faults, than in the upstream part, at the easternmost edge of the Pelagonian massif.

1. Introduction

The central parts of the Balkan Peninsula are dominated by mountainous landscapes with deeply incised valleys, alternating with a number of low relief basins. They are the consequence of the long-term interaction of surface and tectonic processes in this region, starting with the mountain building in Early Cretaceous to Paleogene times and the ongoing Cenozoic extension due to the complex convergence of Africa

* Corresponding author at: Isotope Climatology and Environmental Research Centre, HUN-REN Institute for Nuclear Research (ATOMKI), Bem tér 18/c, 4026 Debrecen, Hungary.
E-mail address: temovski.marjan@atomki.hu (M. Temovski).

https://doi.org/10.1016/j.geomorph.2023.108994
Received 7 June 2023; Received in revised form 16 November 2023; Accepted 17 November 2023
Available online 23 November 2023

and Eurasia. While the general geomorphology of the region is reasonably well understood (e.g., Manakovik et al., 1998; Kolčakovski and Milevski, 2012; Milevski, 2015; Temovski, 2016), information on the Quaternary incision rate of rivers and related tectonic uplift is generally lacking, with only few data available on the timing of landscape evolution (e.g., Pavićević et al., 2016; Temovski et al., 2013, 2016).

Caves, offer a great possibility to reconstruct past landscapes, as their development is largely related to the evolution of the adjacent surface, and their morphology and deposits are well protected from surface erosion (e.g., Ford and Williams, 2007; Palmer, 2007; De Waele and Gutiérrez, 2022). Furthermore, cave deposits can be dated by different geochronological methods (Sasowsky and Mylroie, 2004), thus providing temporal constraints on landscape evolution (e.g., Häuselmann et al., 2015; Bella et al., 2019; Zupan Hajna et al., 2020). Dating of cave deposits related to cave levels that correspond to past valley base levels can also provide an indirect estimation of valley incision rates and related tectonic uplift (e.g., Granger et al., 2001; Häuselmann et al., 2007; Columbu et al., 2015, 2021; Harmand et al., 2017; Pennos et al., 2019; Hill and Polyak, 2020; Sauro et al., 2021; Genuite et al., 2022).

Recent research on cave morphology and sediments in the lower part of Crna Reka river basin (N. Macedonia) identified two major cave development phases: one related to Pliocene-Early Pleistocene basin infilling and establishment of lacustrine environments, and a subsequent cave development phase related to valley incision due to draining of the lacustrine systems and tectonic uplift (Temovski, 2016).

Here, we present new geochronological data from cave deposits in the lower part of the Crna Reka drainage basin that constrain the timing of cave and karst development in the area. This allows us to further constrain the Pleistocene incision of Crna Reka valley and its tributaries, as well as to better understand the landscape evolution and tectonic uplift rates in the region. We apply U-Th dating of speleothems and burial age determination of clastic sediments using the cosmogenic radionuclide (CRN) pair of ^{26}Al and ^{10}Be, the latter applied for the first time in this region.

2. Study area

2.1. An overview of the geomorphology of Crna Reka drainage

Crna Reka (207 km) is one of the longest rivers in N. Macedonia and the second longest tributary to Vardar River (388 km), the main drainage of the central part of the Balkan Peninsula (~25,000 km^2) that flows into the Aegean Sea (Fig. 1). Crna Reka starts at the southern edge of a karstic plateau in the Demir Hisar area, and flows eastward through the Pelagonian, Mariovo and Tikveš basins where it joins the Vardar River (Fig. 2). It has a composite valley that includes low-slope wide sections in the plains of the Pelagonian and Tikveš basins, and deep gorges cutting through Selečka, Kozjak and Dren Mts, and the central plateau of the Mariovo basin (Manakovik and Andonovski, 1984; Temovski, 2016).

The Crna Reka drainage is developed along two major geotectonic zones, the Pelagonian massif in the west, and the Vardar zone in the east (Fig. 2). They are part of the Dinarides-Hellenides orogen that formed due to the convergence of the Adria microplate and the European plate in Late Cretaceous time, with the suture located in the Vardar zone (Schmid et al., 2020). Superimposed onto these geotectonic units are Cenozoic extensional tectonic structures formed as part of the South Balkan extensional regime, the northern segment of the Aegean extensional system (Burchfiel et al., 2008). Two periods of extension were identified (Dumurdzanov et al., 2005; Burchfiel et al., 2008), with the Paleogene Tikveš basin forming in the first one, from the Middle to Late Eocene. This was followed by Oligocene-Early Miocene shortening. During the second extensional period, from the Early Miocene to the present, the Pelagonian basin started to form in the Middle to Late Miocene and Tikveš and Mariovo basins were initiated in the Late Miocene (Dumurdzanov et al., 2005).

Landscape evolution in the Crna Reka drainage is related to the

Fig. 1. Location of the Vardar River drainage basin (purple outline) in the central parts of the Balkan Peninsula. V – Vardar River, CR – Crna Reka, O – Ohrid Lake.

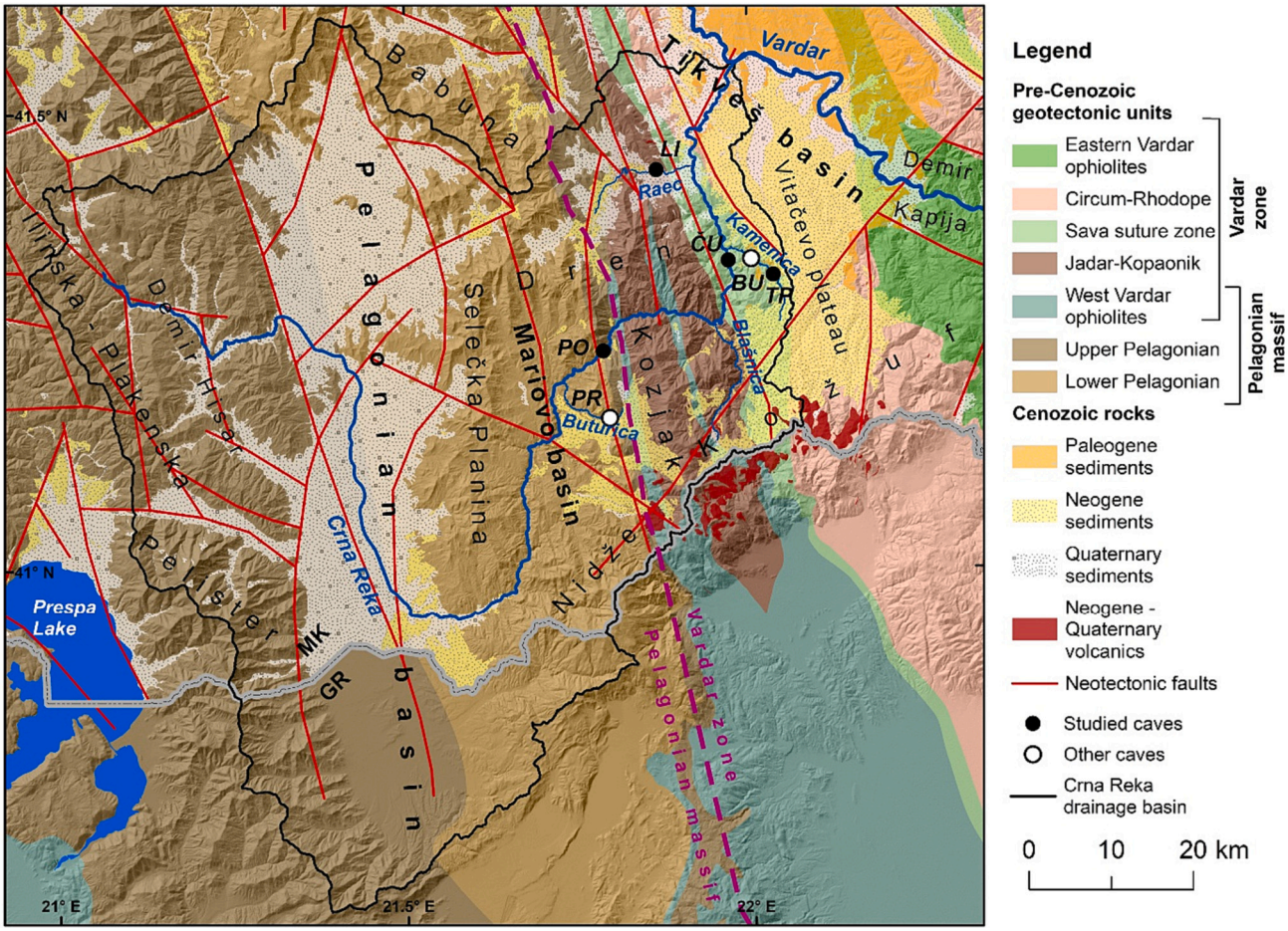

Fig. 2. Geological setting of the Crna Reka drainage and location of the studied caves. Pre-Cenozoic geotectonic units after Schmid et al., 2020. Distribution of Cenozoic lithology and neotectonic faults are from Arsovski (1997) and cover only the Macedonian part of the drainage. BU – Budimirica Cave, ČU – Čulejca Cave, LI – Liljarnikot Cave, PO – Podot Cave, PR – Provalata Cave, TP – Temna Peštera Dragožel.

evolution of the Neogene-Quaternary basins, whose sediments indicate mostly lacustrine to fluvial environments in the Late Miocene to Early Pleistocene (Dumurdzanov et al., 2004). Two periods of valley incision can also be identified, the first one at the end of Miocene and the second one from Early or Middle Pleistocene to present (Temovski, 2016). The valley incision at the end of Miocene is likely related to the effect of the Messinian Salinity Crisis, with evidence of its influence identified along the central parts of the Balkan Peninsula (Clauzon et al., 2008; Suc et al., 2015). Pliocene sediments found along the Crna Reka valley between the Mariovo and Tikveš basins (Fig. 1; Dumurdzanov et al., 2004) support the Miocene age of the paleo-Crna valley. The current drainage network of Crna Reka and its tributaries was established after the draining of the Mariovo Lake (in the Mariovo Basin) and the Central Macedonian Lake (in the Tikveš Basin), linked to subsidence in the Aegean Sea (Dumurdzanov et al., 2004; Temovski, 2016). The onset of the draining is considered to have happened in the Early Pleistocene (>1.6 Ma) in the Mariovo basin (Temovski et al., 2013), while the natural barrier at Demir Kapija (400–440 m asl), the southeastern edge of the Tikveš basin (Fig. 2), was breached by the Early to Middle Pleistocene (Dumurdzanov et al., 2005).

Base-level changes in the lower part of Crna Reka drainage, from incision of deep valleys, to their thick aggradation and later again incision, had a major effect on karst development in the area, both epigene and hypogene. Morphological and sedimentological studies of caves in the area identified karst and cave development related to each of these phases (Temovski, 2016). However, chronological data is available only from a few caves. An Early Pleistocene (1.60 ± 0.05 Ma) age was obtained for the sulfuric acid phase in Provalata Cave from Ar-Ar dating of speleogenetic alunite (Fig. 2; Temovski et al., 2013). A Late Pleistocene age (≤83 ± 15 ka) was determined for the cave deposits in Budimirica Cave using a combination of paleomagnetic and U-Th dating (Fig. 2; Temovski et al., 2016). A preliminary age of >350 ka was obtained by U-Th dating of flowstone from Temna Peštera – Dragožel (Fig. 2; Temovski et al., 2016).

2.2. General characteristics of the studied caves

2.2.1. Liljarnikot Cave

The Liljarnikot Cave is a small (70 m) cave, not reported previously in the literature, located in the Drenovo gorge in the Raec valley, a left tributary to Crna Reka that drains the small Raec basin (Figs. 2, 3). The Drenovo gorge is a superimposed valley that developed in the Upper Cretaceous rocks after cutting through the Pliocene-Pleistocene cover. Three caves are found in the gorge: Galabarnikot, located 148 m above the riverbed; Liljarnikot, 63 m above the riverbed; and the Quarry cave, a vertical cave section opened by quarrying, with an entrance located ~25 m above the current riverbed.

2.2.2. Temna Peštera – Dragožel Cave

The Temna Peštera – Dragožel Cave is located in the middle part of the Kamenica valley, and corresponds to a river terrace at 550 m asl, and ~80 m above the current river bed (Fig. 3). The cave is developed in Late Cretaceous limestone, with passages mostly formed along prominent fractures with a WSW-ENE direction. Detailed descriptions of the

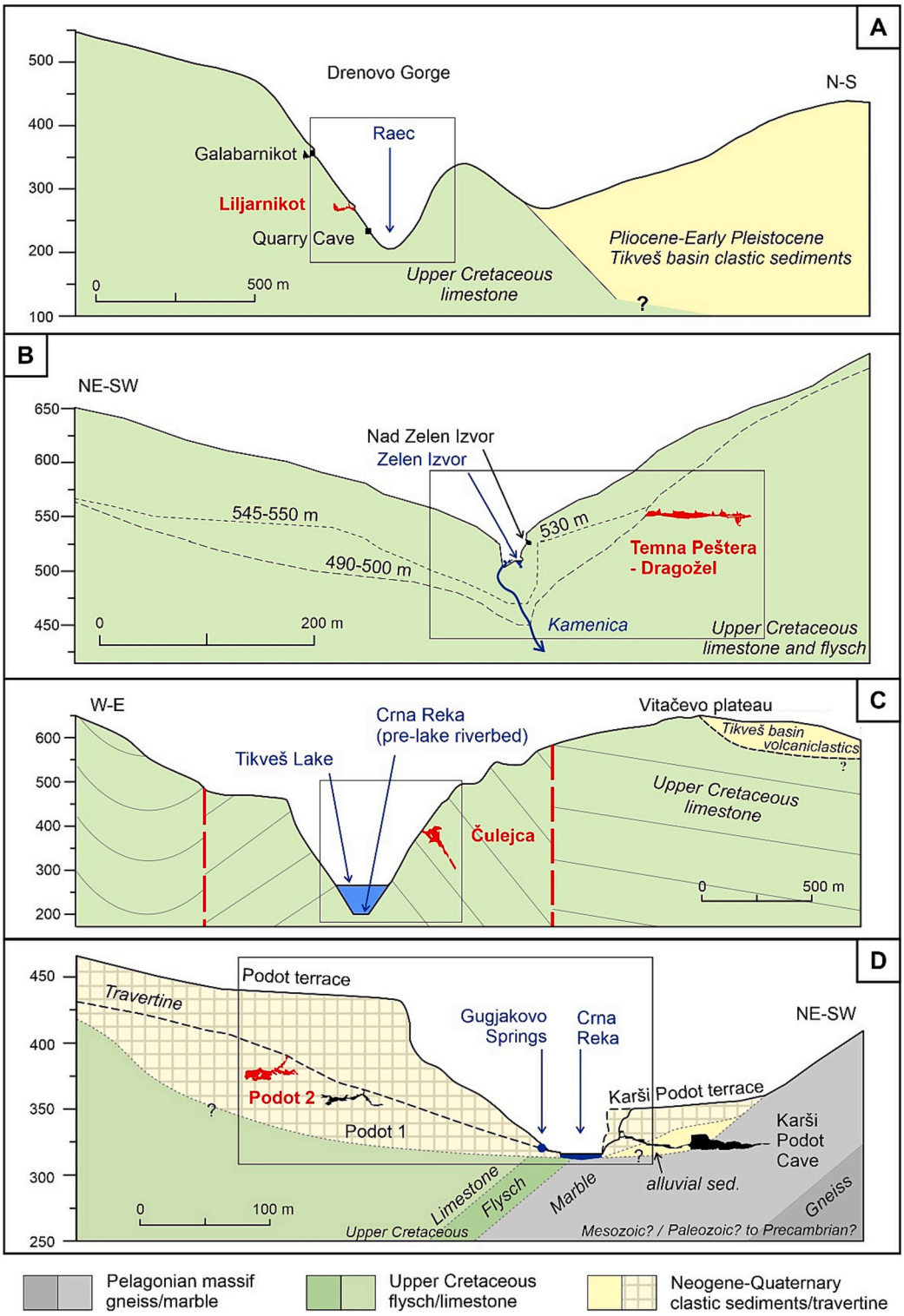

Fig. 3. Valley cross-sections and the relationship of the studied caves to the local geomorphological setting. A – Liljarnikot Cave in the lower part of Raec valley (Drenovo Gorge); B – Temna Peštera – Dragožel in the middle part of Kamenica valley, with nearby valley cross-sections with river terraces and caves (Zelen Izvor and Nad Zelen Izvor); C – Čulejca Cave in the lower part of Crna Reka valley (NW edge of Vitačevo plateau). The modern Crna Reka riverbed is submerged under the artificial reservoir forming Tikveš Lake. Note that the indicated strata dip is an apparent dip adjusted to the W-E projection of the cross-section; D – Podot 2 Cave in the Podot locality, with two major travertine terraces, Podot and Karši Podot and nearby caves (Podot 1 Cave, Karši Podot Cave). Rectangles show a more detailed perspective of the altitudinal relationships between the studied caves and the present river thalweg in Fig. 11.

morphology, cave sediments and speleogenesis are given in Temovski (2016). Temna Peštera – Dragožel is ~125 m long and mostly horizontal, with an ~8 m deep sump in its upstream part (Fig. 4). The sump turns horizontal at the bottom and is filled mostly with clay, with sand in some places. Remnants of fine-grained clastic sediments (mostly brown silt and dark brown clay) can be found elsewhere in the upstream part, associated with a paragenetic morphology (e.g., half-tube channels). They are similar to the sediments found in other caves throughout the

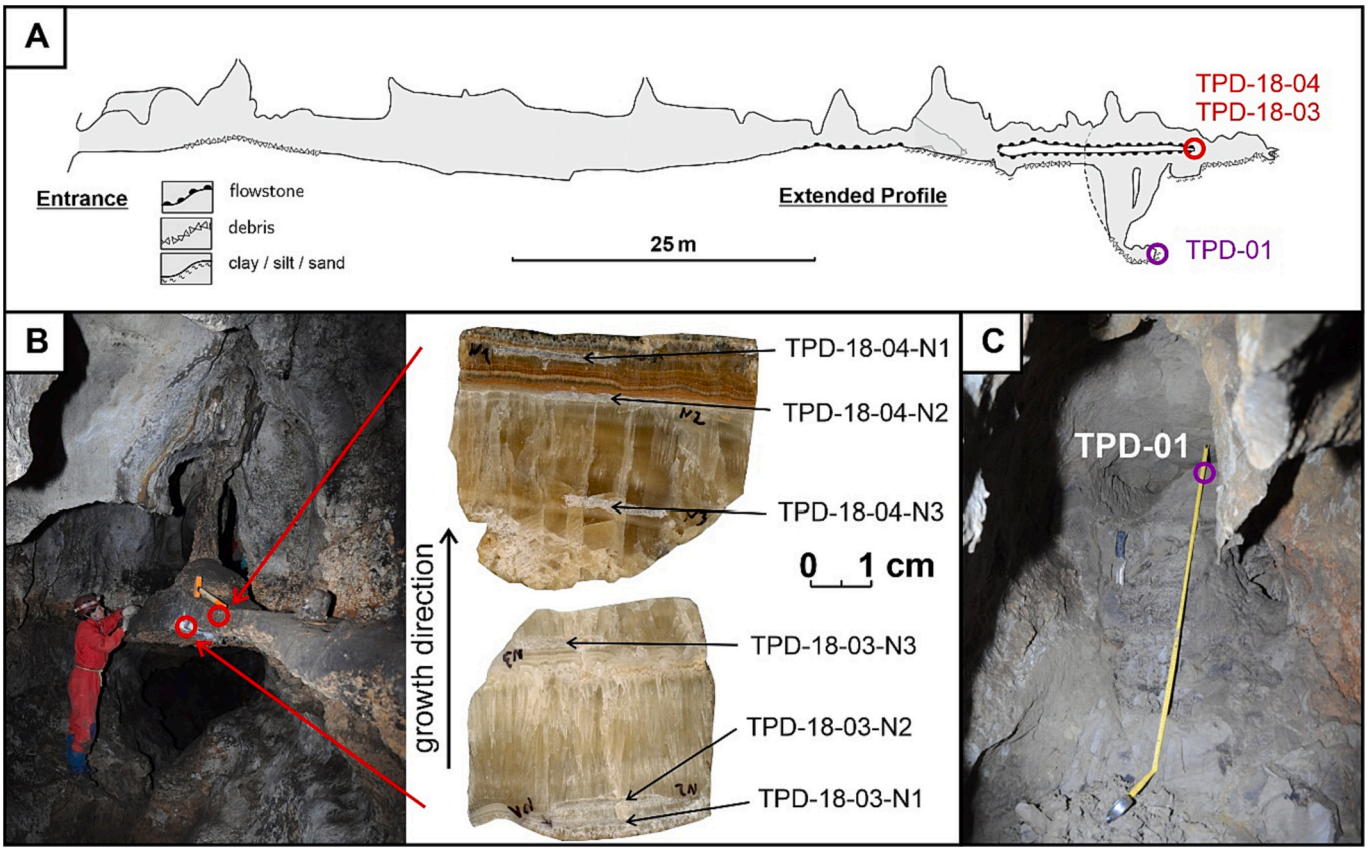

Fig. 4. Location of the samples collected from Temna Peštera – Dragožel. A – Location of the samples on the extended profile map of the cave; B – view of the flowstone false-floor and close-up of the collected top and bottom part flowstone samples with indicated position of the subsamples for U-Th dating; C – view of the sediment filled sump, and the profile from which the sample for cosmogenic burial age dating was collected.

Kamenica valley, sourced from the volcaniclastic deposits of the Vitačevo plateau (Temovski, 2016). Temna Peštera – Dragožel formed in a shallow phreatic to epiphreatic environment, with its clastic sediment infilling and paragenetic morphology developed in the inner part related to the aggradation in the Kamenica valley, likely corresponding to the terrace at 550 m (Temovski, 2016). Subsequent incision in the Kamenica valley, led to the lowering of the water table. This was followed by partial removal of sediments and deposition of thick flowstone deposits. Further base-level lowering led to incision of small vadose channels and removal of the sediments below the flowstone deposit, creating a flowstone-covered false floor. Preliminary U-Th dating of the flowstone indicated that it is older than 350 ka (Temovski et al., 2016).

2.2.3. *Čulejca Cave*

The Čulejca Cave is located in the lower part of the Crna Reka drainage, on the right side of a ~300 m deep valley where the Crna Reka cuts across the NW part of the Vitačevo Plateau (Figs. 2, 3). The cave is developed into Late Cretaceous limestone, exposed after the removal of the Neogene-Pleistocene volcaniclastic cover of the Vitačevo Plateau. It is ~600 m long and ~100 m deep, with large tube-like phreatic passages generally rising southward along NW-dipping bedding partings and SW-NE oriented fractures (Fig. 5). Detailed descriptions of the cave morphology, sediments and speleogenesis are given in Temovski (2016). The main cave passage formation, based on passage organization, paragenetic morphology and distribution of fine-grained sediments was related to base-level rise, attributed to Pliocene sedimentation in the Tikveš basin that eventually led to complete covering and fossilization of the karst system. The per ascensum cave development implies a prior karstification phase related to base-level lowering. This was hypothesized to be due to valley incision at the end of the Late Miocene, likely related to the influence of the Messinian Salinity Crisis (Temovski, 2016). The Pleistocene incision of Crna Reka triggered cap-rock retreat and reactivation of the karst system that led to removal of fine-grained sediments in the cave and widespread deposition of subaqueous speleothems (mammillary calcite, pool fingers, cave rafts), that at places transition to flowstone. Past water table markers can be found as water-level marks in mammillary speleothems or as alluvial notches related to back-flooding of Crna Reka (Fig. 5A, C).

2.2.4. *Podot 2 Cave*

The Podot area is characterized by two terraces composed of travertine deposits (tufa, tufaceous limestone, carbonate breccia and conglomerates), deposited on top of Pre-Cenozoic nappe structures of gneiss marble, flysch and limestone (Figs. 2, 3). The higher, Podot terrace (440 m asl) is on the left valley side, while the lower Karši Podot terrace (350 m asl) is on the right valley side, with the current Crna Reka riverbed at 320 m asl. An active thermal cave is found in the Karši Podot terrace, while numerous cave openings with two explored caves, Podot 1 and Podot 2, are found in the Podot terrace (Temovski, 2016). The Gugjakovo springs (Temovski et al., 2021), a group of lukewarm springs, are found below them, some 5 m above the current riverbed. Podot 2 is a fissure cave developed mainly along fractures with a SW-NE and NW-SE direction. The passages are generally taller than they are wide with a phreatic morphology. Podot 2 has two horizontal levels, with mammillary speleothems covering the passage walls in the lower level, while the upper level is generally affected by collapses (Fig. 6). It is a fossil phreatic cave with the Gugjakovo springs as the current discharge point of this system. Its evolution is connected with the incision of Crna Reka that controlled the lowering of the water table (Temovski, 2016).

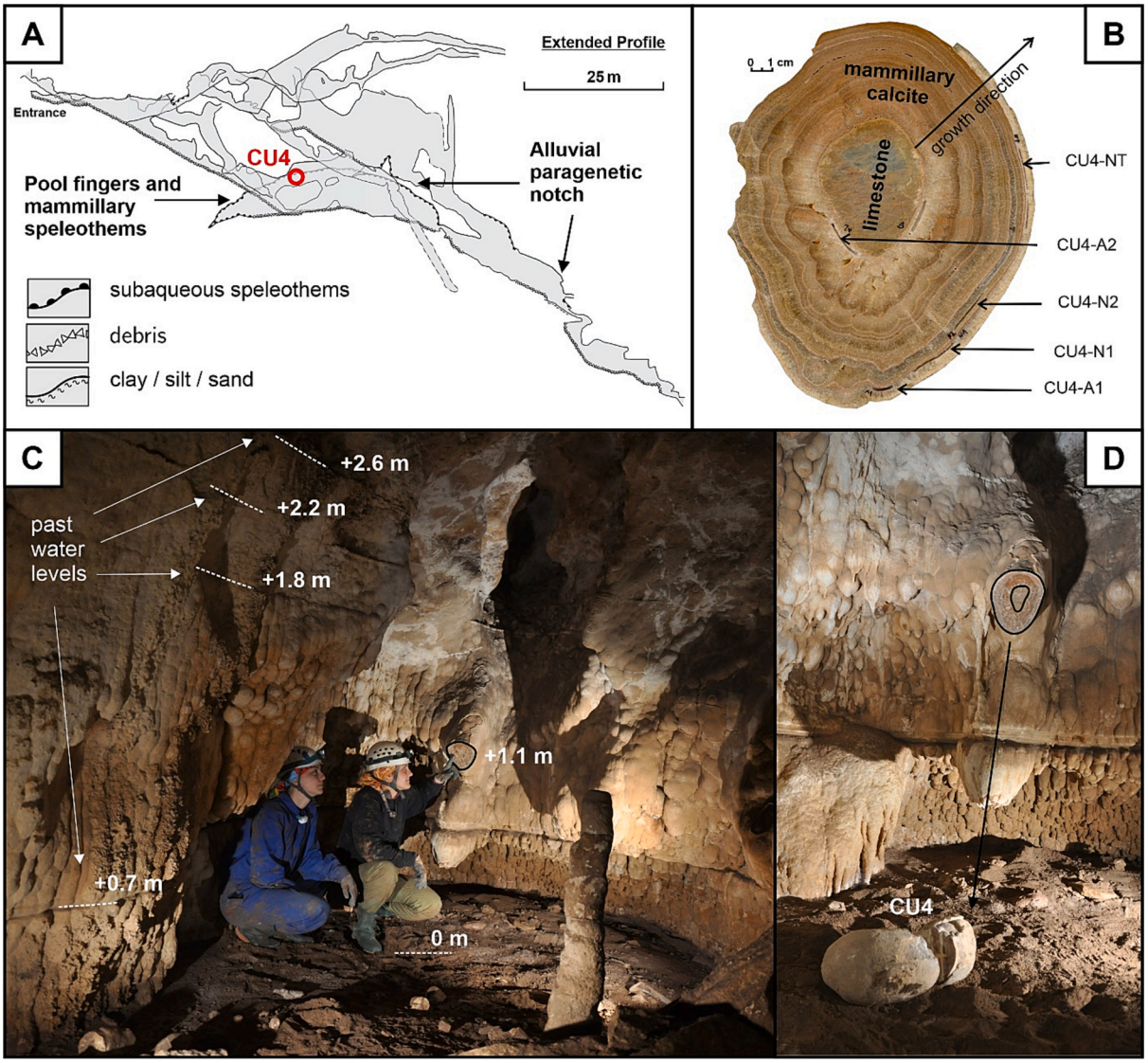

Fig. 5. Location of the sample collected from Čulejca Cave. A – Location of the samples on the extended profile map of the cave. Note indication of large extent of subaqueous deposits in the middle part of the cave and two alluvial paragenetic notches; B – cut surface of the sampled speleothem showing layering in the mammillary calcite, with indicated position of the subsamples for U-Th dating, and a limestone pendant in the center; C – view of the niche where the sample was collected, covered by subaqueous speleothems with several water level marks and their position above the current floor. D – Close-up showing the broken face on the wall and the fallen piece of the mammillary-calcite-coated pendant from which CU4 sample was collected.

3. Methodology

3.1. Cave mapping, sampling and sample description

Detailed field mapping of Liljarnikot Cave was undertaken at 1:100 scale using a Leica laser distance meter (Disto D3) and Suunto compass (Suunto KB-20). Field data (sketches, measurements) were later processed in Therion cave mapping software (Budaj and Mudrak, 2008), to produce cave maps in plan and extended profile views. Morphogenetic analysis and speleogenetic interpretation were undertaken based on the resulting detailed map and field observations. Additionally, a sample for U-Th dating was collected from the base of the flowstone deposit covering remnants of clastic sediments in the horizontal section of the inner part of the cave (Figs. 7, 8B).

At Temna Peštera – Dragožel, for CRN burial dating, sandy to silty sediment (TPD-01) was collected from the upper parts of the sediment profile in the horizontal section of the sump in the upstream part, approximately 60 m below the surface. Above the sump, a flowstone plaque (false floor) is found, 15 to 30 cm thick, with the thickest part in the middle, above which it continues upwards into a dripstone column up to the ceiling (Fig. 4B). On the bottom side boxwork speleothems can be seen with some clay remnants. Samples from the bottom (TPD-18-03) and top (TPD-18-04) part of the flowstone false floor were cut by a battery-operated diamond saw. TPD-18-03 sample is composed of yellowish columnar calcite with some layering noticeable near the bottom and the top of the sample. TPD-18-04 sample has a similar composition, except for the topmost 1 cm where clayey layers are found and finishes with a black coating that is ubiquitous on the passage floor, probably due to fire burning in the cave. Three subsamples for U-Th dating were collected from both the bottom and top sample, sampled within ~3 cm from the bottom and top surface, respectively.

At Čulejca, in a small niche in the middle part of the cave (Fig. 5), a sample was collected (CU4) from a broken piece of mammillary speleothem, that was found fallen from the wall. The original sample position was 1.1 m above the floor. The CU4 sample is ~60 mm thick, with a limestone pendant in the middle. It shows strong banding with intervening calcite and clay layers, with clayey parts diminishing downwards, and at least 5 prominent clay layers (Fig. 5B). The outermost

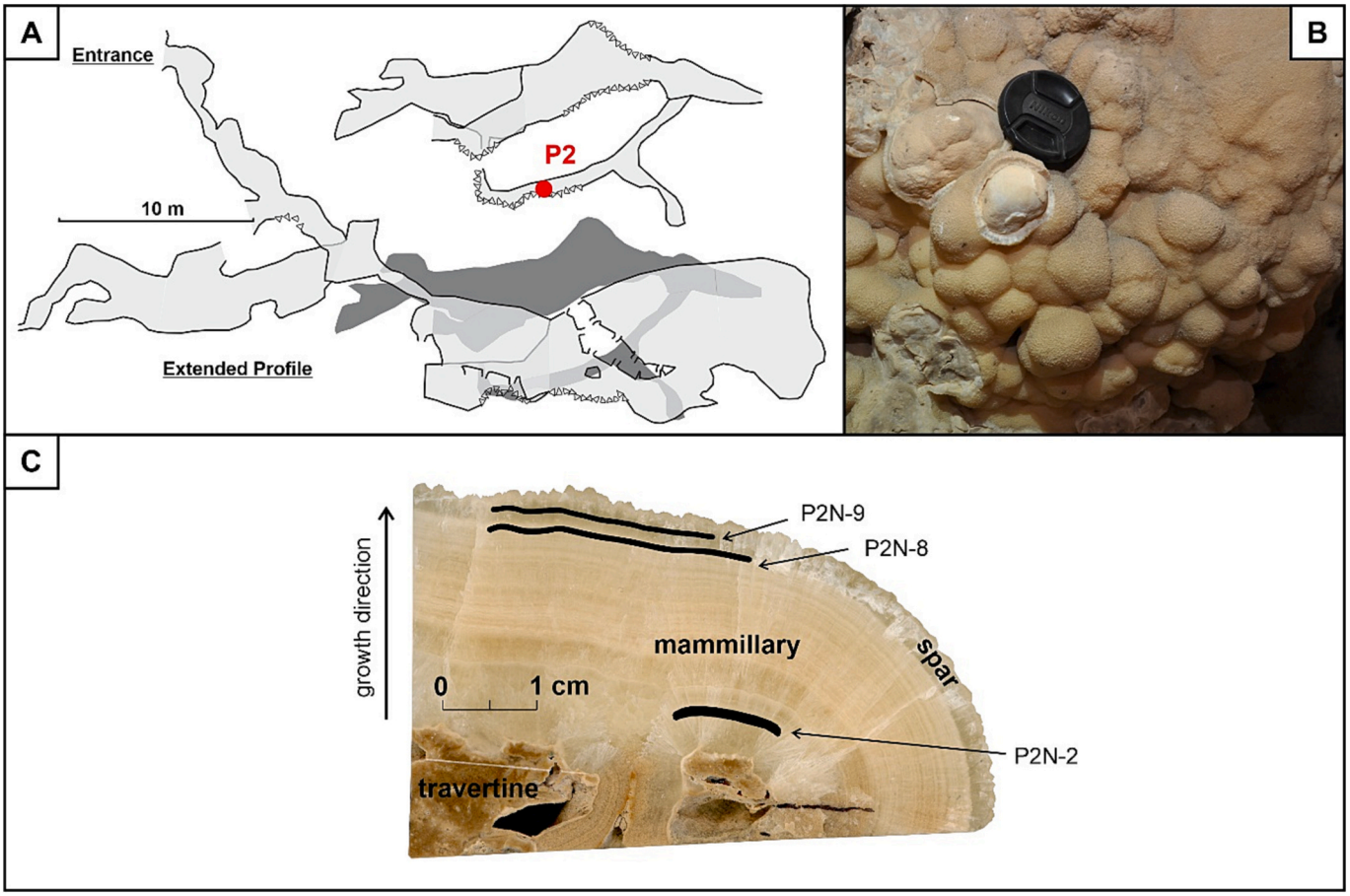

Fig. 6. Location of the sample collected from Podot 2 Cave. A – Location of the sample on the extended profile map of the cave. B – View of the mammillary speleothems on the wall in the passage where P2 samples were collected. C – Cut surface along growth axis of the sample with indicated position of the subsamples for U-Th dating.

layer is quite porous due to subsequent weathering. Above the CU4 location at least three noticeable water-table marks are found (+1.8 m, +2.2 m, +2.6 m above the floor) with lateral speleothem growth (shelfstone), while one strong water-table notch is found below CU4 (+0.7 m above the floor) that cuts through the mammillary deposits (Fig. 5C). CU4 deposition is likely coeval with the water-table marks above. The clay is likely redeposited from higher elevations by vadose drip waters. Five samples were collected for U-Th dating from the bottom and top layers of the CU4 sample, with an attempt to constrain the age of onset and termination of speleothem deposition (Fig. 5B). As the top surface of the mammillary coating in CU4 sample appeared altered, three subsamples (CU4-A1, CU4-N1, CU4-NT) were collected from the same layer, ~5 mm from the top, where the calcite appeared somewhat denser. An additional top sample (CU4-N2) was collected at ~10 mm from the top, and a bottom sample (CU4-A2) was collected at ~3 mm from the bottom of the section.

At Podot 2, a piece of mammillary speleothem (P2) fallen from the wall was collected in a side passage in the lower parts of the cave (Fig. 6). The subaqueous speleothem is ~25 mm thick, with the bottom ~20 mm composed of densely laminated, mammillary calcite, and the outer ~5 mm with a calcite spar layer (Fig. 6C). Three samples were collected for U-Th dating, two near the bottom (P2N-2) and top (P2N-8) part of the mammillary section, and one (P2N-9) from the spar layer.

3.2. Burial age dating of cave sediments

The burial age determination method using in situ produced cosmogenic radionuclides (CRN) considers the concentrations and ratio of cosmogenic ^{26}Al and ^{10}Be in sedimentary quartz grains. During their pre-burial history, surface sediments accumulate cosmogenic nuclides in an amount inversely proportional to the source denudation rate but at a constant ^{26}Al/^{10}Be ratio (Granger, 2006). After their deposition (burial) as allogenic sediments in a cave, the CRN production stops, and the CRN concentrations start to decrease due to radioactive decay. The half-life of ^{10}Be (1.387 ± 0.012 My; Chmeleff et al., 2010; Korschinek et al., 2010) is roughly double that of ^{26}Al (0.705 ± 0.017 My, Nishiizumi, 2004), therefore the initial nuclide ratio will start to decrease. This decrease of the nuclide ratio can be used for the determination of the burial duration of the sample (Granger, 2006, 2014).

The studied cave sediment sample (TPD-01) was dominated by fine sand (100–250 μm, 44 %), followed by the silt fraction (2–50 μm, 34 %), with clay, very fine sand and medium sand (250–500 μm) representing only 7 %, 8 % and 7 %, respectively. Accordingly, the sample was wet sieved and grain-size fraction above 125 μm was used for burial age determination.

Sample processing was performed at the Cosmogenic Nuclide Sample Preparation Laboratory of the Institute for Geological and Geochemical Research (Budapest, Hungary), following the procedures of Merchel and Herpers (1999) and Merchel et al. (2019) as described in Ruszkiczay-Rüdiger et al. (2021). The stable ^{27}Al was determined using Microwave Plasma – Atom Emission Spectrometry (Agilent 4100 MP-AES) at the Isotope Climatology and Environmental Research Centre, Institute for Nuclear Research (Debrecen, Hungary). AMS (Accelerator Mass Spectrometry) measurements of the isotopic ratios of the samples were carried out at the Vienna Environmental Research Accelerator (VERA), Faculty of Physics, University of Vienna, Austria. The ^{26}Al/^{27}Al ratio was

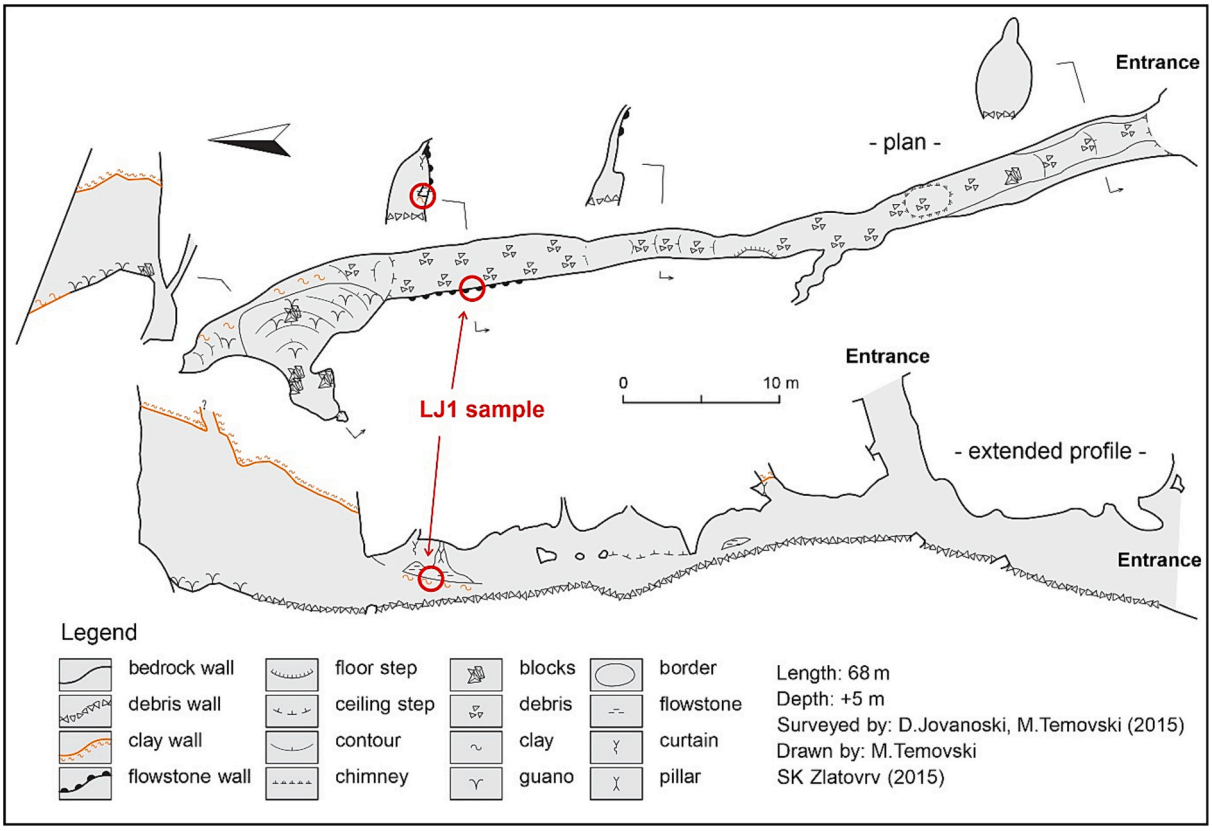

Fig. 7. Detailed map of Liljarnikot Cave with location of the collected flowstone sample.

measured with the ILIAMS method, where the more prolific AlO^- beam is injected into a radiofrequency quadrupole ion guide, suppressing the magnesium isobar by 14 orders of magnitude (Lachner et al., 2021), and normalized to SMD-Al-11 ($^{26}Al/^{27}Al = (9.66 \pm 0.14) \times 10^{-12}$; Rugel et al., 2016). The $^{10}Be/^{9}Be$ ratio was measured using the foil stack absorber technique described in Steier et al. (2019), and normalized to SMD-Be-12 ($^{10}Be/^{9}Be = (1.704 \pm 0.030) \times 10^{-12}$; Akhmadaliev et al., 2013).

First, the simple burial age was calculated using the eq. (6) of Granger and Muzikar (2001). This method is supposed to provide a reasonable age estimate for samples completely shielded from cosmic radiation. The 60 m depth of the TPD-01 sample is sufficient to be completely shielded from cosmic radiation. However, for a more precise age determination that might consider post-burial CRN production and can provide an estimate on the source and sink denudation rates (the latter only in the case of incomplete burial), the burial duration was also calculated using the equation of Braucher et al. (2011), where the three main types of secondary cosmic ray particles penetrating the lithosphere (neutrons, negative muons and fast muons) are considered (with attenuation lengths of L_n: 160 g/cm^2; $L_{\mu slow}$: 1500 g/cm^2; $L_{\mu fast}$: 4320 g/cm^2; Gosse and Phillips, 2001; Heisinger et al., 2002a, 2002b). Rock density was taken as 2.6 g/cm^3 both at the source and the sink. The spallogenic production rate of ^{10}Be and ^{26}Al was scaled to the sample location using the Lal (1991)/Stone (2000) time independent scaling from sea level at high latitude (SLHL) production rate of ^{10}Be of 4.01 ± 0.33 atoms/g SiO_2/yr (Borchers et al., 2016). CosmoCalc add-in for Excel (Vermeesch, 2007) has been used to convert sample elevations to atmospheric pressures and to calculate the scaled production rate. The spallogenic production rate ratio of $^{26}Al/^{10}Be$ used for the age calculations was 6.7 ± 0.6 (Fenton et al., 2022). Muogenic production rates at the sample location were estimated based on the procedures of Heisinger et al. (2002a, 2002b) updated by Balco (2017), using the code published by Nørgaard et al. (2023). Geographic data (e.g., cave entrance coordinates) used for the age calculation are available upon request.

3.3. U-Th dating of speleothems

U-Th (or ^{230}Th) dating of speleothems is based on the extreme fractionation of U and Th in groundwater, with U being easily soluble and Th having extremely low solubility. As a result, the crystal lattice of the speleothems incorporates U, but only negligible amounts of ^{230}Th. Thus, if the crystal lattice remains a closed system, the time passed since speleothem deposition can be determined based on the radioactive evolution of ^{238}U, ^{234}U, and ^{230}Th (Edwards et al., 1987; Dorale et al., 2007; Cheng et al., 2013).

Collected speleothem samples were cut, grinded and polished. Subsamples for U-Th dating were drilled using a Dremel handheld drill along the sample growth axis. About 10 mg of carbonate powder was first collected for determination of U concentration on an Agilent 8800 Triple Quadrupole ICP-MS. Based on the U concentration, about 20–150 mg of sampled carbonate powder was then collected for U-Th dating.

Chemical preparation to separate U and Th fractions from the carbonate matrix was carried out in a Class 1000 clean laboratory, with procedures similar to those described in Edwards et al. (1987). Briefly, samples were first dissolved in concentrated nitric acid and spiked with a ^{229}Th–^{233}U–^{236}U tracer (a mixture of the IRMM-3636a and the SRM 4328C reference materials), with an amount based on the predetermined U concentration. Separation of U and Th fractions were done in a column filled with UTEVA resin. The thorium fraction was collected with 4 M hydrochloric acid, and the uranium fraction with 0.1 M hydrochloric acid. They were evaporated to dryness and followed by several cycles of digestion in concentrated nitric acid and evaporation to dryness, after which the U fraction was collected in 3 % nitric acid and the Th fraction in a mixture of 3 % nitric acid and 0.05 M hydrofluoric acid.

The isotope ratio measurements were carried out on a Neptune PLUS

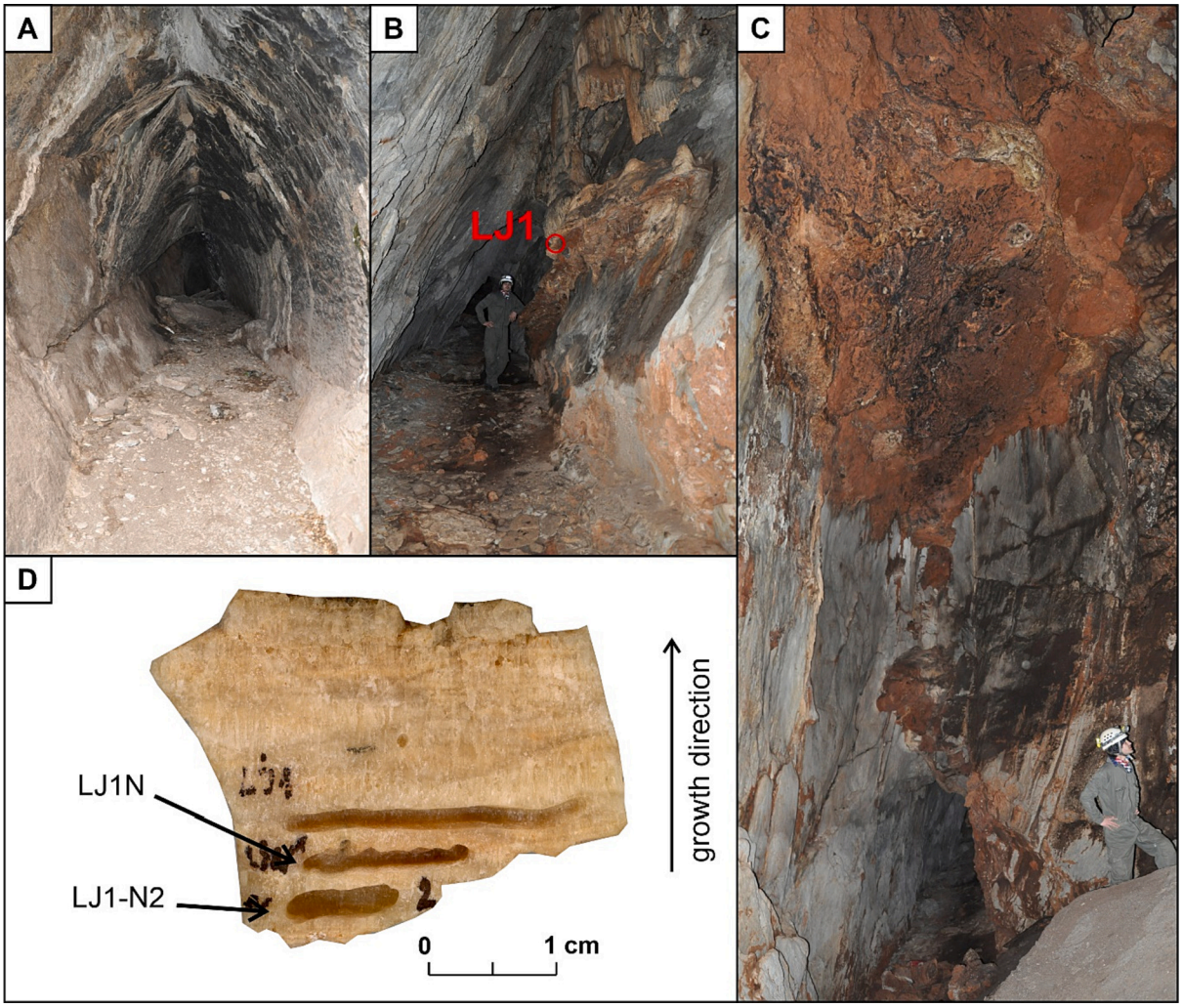

Fig. 8. Characteristic parts in Liljarnikot Cave. A – Phreatic morphology close to the entrance of the cave. B – Flowstone deposits with remnants of clastic sediments at its base standing above the current passage floor. Location of the collected sample is indicated. C – Panoramic view of the shaft in the inner part clogged with clay sediments at the ceiling. Note the side continuation to the horizontal section of the cave. D – Cut side of the sampled flowstone, with indicated positions of the subsamples for U-Th dating.

multicollector ICP mass spectrometer equipped with an Aridus 3 desolvating system. For the measurement of uranium isotopes (^{233}U, ^{234}U, ^{235}U, ^{236}U, ^{238}U), only Faraday-cups were used to determine the ion beam intensities. For thorium isotopes (^{229}Th, ^{230}Th, ^{232}Th), the uranium detector configuration was used in a way that thorium ion beams were aligned to the detectors with the dispersion quadrupole of the MC-ICPMS. The secondary electron multiplier in the central position was used for the ^{230Th}, and with a magnet jump for the ^{229}Th isotopes. A laboratory standard solution (StalMix) prepared from the CRM 112-A reference material and the IRMM-3636a double uranium spike (^{233}U/^{236}U = 1.01906 ± 0.00016) was used during the isotope ratio measurements for the standard-sample bracketing. The mass bias correction for U and Th in each sample solution was determined based on the uranium isotope measurement run using the known ^{235}U/^{238}U isotopic ratio of CRM 112-A.

All preparation procedures and analyses were carried out at the Isotope Climatology and Environmental Research Centre, Institute for Nuclear Research (Debrecen, Hungary).

The U-Th ages were calculated by iteration using the standard ^{230}Th/^{238}U equation (Kaufman and Broecker, 1965; Edwards et al., 1987).

$$\left[\frac{^{230}Th}{^{238}U}\right] = 1 - e^{-\lambda_{230}T} + \left(\frac{\delta^{234}U_m}{1000}\right) \times \left(\frac{\lambda_{230}}{\lambda_{230} - \lambda_{234}}\right) \times \left(1 - e^{(\lambda_{230} - \lambda_{234})T}\right)$$

where the values in square brackets are activities, $\delta^{234}U_m$ is the measured ^{234}U/^{238}U activity ratio expressed as $\delta^{234}U_m = ([^{234}U/^{238}U] - 1) \times 1000$, T is the age and λ's are the decay constants: $\lambda_{238} = 1.55125 \times 10^{-10}$ (Jaffey et al., 1971), $\lambda_{234} = 2.82206 \times 10^{-6}$ (Cheng et al., 2013), $\lambda_{230} = 9.1705 \times 10^{-6}$ (Cheng et al., 2013). The initial ^{234}U/^{238}U ratio ($\delta^{234}U_i$) is calculated from:

$$\delta^{234}U_i = \delta^{234}U_m \, e^{\lambda_{234}T}$$

Detrital Th-corrected ages are calculated by correcting the measured ^{230}Th/^{238}U ratios based on ^{232}Th as an index of the initial ^{230}Th contamination using the following equation (Richards and Dorale, 2003):

$$\left[\frac{^{230}Th}{^{238}U}\right]_{corr} = \left[\frac{^{230}Th}{^{238}U}\right] - \left[\frac{^{232}Th}{^{238}U}\right] \times \left[\frac{^{230}Th}{^{232}Th}\right]_i \times \left(e^{-\lambda_{230}T}\right)$$

where $[^{230}Th/^{232}Th]_i$ is the activity ratio of the detritus at the time of formation, for which bulk earth ^{230}Th/^{232}Th atomic ratio of 4.4 ± 2.2 × 10^{-6} was used. Calculated U-Th ages are reported in thousand years Before Present (ka BP), with Present defined as the year 1950 CE Age

uncertainties are given at 2σ, and incorporate analytical uncertainties and uncertainties in ratios of reference materials.

4. Results

4.1. Morphology and cave deposits of Liljarnikot Cave

Liljarnikot cave is 70 m long and has mainly one horizontal N-S oriented passage with a main entrance that opens at the valley side, and another entrance shaft joining some 20 m inward (Fig. 7). It is developed along the strike direction of steeply dipping Turonian limestone. Despite its general horizontal extension, there are at least three sections of the cave that have vertical vadose passage morphology: the entrance shaft, a small clay-choked chimney further inward, and the innermost section (room) that is 5–10 wide and up to 10 m high, with a clay-choked ceiling and floor covered with clay breakdown and guano (Figs. 7, 8).

These vertical sections are connected by horizontal sections with phreatic morphology. They are partly modified by subsequent breakdown, that, due to the steep strata dip, covers the floor with small platy rock debris. The western wall of the passage south from the large vertical section is covered with dripstone and flowstone that hangs above the floor from about 2 m down to 0.5 m towards the south (Figs. 7, 8B). At the base of the flowstone remnants of clastic sediments (mainly clay, but also some breccia with limestone fragments) are found.

4.2. Burial age results

Analytical data and cosmogenic ^{10}Be and ^{26}Al concentration of the TPD-01 sample from Temna Peštera – Dragožel are given in Table 2. The ^{9}Be carrier type was Phena EA (2246 ± 11 μg/g; Merchel et al., 2013). Due to the high natural Al content of the sample, no ^{27}Al carrier was added. The blank ^{10}Be/^{9}Be ratio was (4.85 ± 0.50) × 10^{-15}; and the blank ^{26}Al/^{27}Al ratio was (7.87 ± 4.86) × 10^{-16}. The reported uncertainties comprise the analytical uncertainties (internal uncertainty), as well as the uncertainties of the half-lives of ^{10}Be and ^{26}Al, the spallogenic production rate of ^{10}Be, the spallogenic production rate of the ^{26}Al/^{10}Be ratio and the rock density (external uncertainty).

Burial ages and uncertainty estimates are given in Table 3. The simple burial age assuming complete burial and spallogenic CRN production only, was estimated at 2.08 ± 0.38 Ma. The burial age accounting for all production pathways and sample depth is 2.12 ± 0.47 Ma. The estimated source denudation rate is 0.04 ± 0.01 m/ka, a temporal rate relevant for the time when the sediment was eroded (i.e., 2.12 ± 0.47 Ma). The two burial ages are statistically identical, and in a following section the latter will be discussed as the most probable time when the sediment was eroded and buried in the cave.

4.3. U-Th results

U-Th dating was carried out on 16 subsamples from the five speleothem samples collected in the studied caves. U-Th ages were obtained for 12 samples (Table 4).

At Liljarnikot, U-Th dating was done on two subsamples from the bottom part of the flowstone, collected close to each other, that gave ages of 146 ± 5 ka (LJ1N) and 121 ± 2 ka (LJ1-N2), that are not in stratigraphic order (Fig. 8D). A possible explanation is that these ages might have been affected by an open system behavior of U, as the sample appeared somewhat weathered. Furthermore, considering the paleoclimate conditions, the younger age, indicating deposition during the MIS 5e interglacial, is more likely than the older one. An age of ~146 ka would imply deposition during the last stages of the MIS 6 glacial period, that based on the paleoclimate record of Ohrid Lake (Fig. 1) was characterized by very cold and dry conditions (Sinopoli et al., 2019), that are unfavorable for speleothem formation.

The three subsamples from the bottom part of the flowstone plaque at Temna Peštera – Dragožel, gave ages that are not in the stratigraphic order, and partly overlap due to their large uncertainty (Fig. 4B). We consider the sample with the youngest age (TPD-18-03-N1; 416 ± 39 ka) as most reliable, with the other ages probably shifted to older ones due to alteration. In the top part, similarly, three samples were collected (Fig. 4B). Age calculation was possible for only one of them (TPD-18-04-N1; 333 ± 21 ka), with the other two having ^{230}Th/^{238}U and δ^{234}U values that fall beyond the infinite age range, reflecting alteration.

From the mammillary calcite at Čulejca Cave, the bottom U-Th sample (CU4-A2) gave an age of 363 ± 16 ka and the one at ~10 mm from the top (CU4-N2) gave 336 ± 22 ka. From the topmost layer, no age was calculated for two samples, clearly affected by alteration, while the third one (CU4-A1) gave the oldest age (543 ± 86 ka). Considering that the inner two samples are in stratigraphic order, and the altered character of the topmost layer, this age was excluded from further interpretation.

Three U-Th ages were obtained from the mammillary speleothem from Podot 2 Cave that allow us to constrain the timing of its deposition as a marker of a former water table (Fig. 6, Table 4). Two samples are from the mammillary section, having U-Th ages of 239 ± 5 ka (P2N-2) and 222 ± 6 ka (P2N-8), and one (P2N-10) from the spar section, with a U-Th age of 164 ± 2 ka.

5. Discussion

5.1. Speleogenesis of Liljarnikot Cave

The cave morphology and sediment distribution at Liljarnikot Cave indicate that the cave formed first as series of parallel shafts, that were later completely filled up with sediment (Fig. 9). Based on the regional setting, the vadose development might have been related to a former base level prior to the deposition of the Pliocene-Pleistocene cover, that subsequently led to base-level rise and filling up of cave passages with sediments. The interpretation of karst development related to a former base level prior to the development of the Drenovo Gorge is also supported by the similar large vertical section in the Galabarnikot Cave, as well as the sediment and flowstone filled vertical Quarry Cave (located ~25 m above the current riverbed), and their location (partly intercepted by the retreat of the valley side). A pre-Pliocene vertical karst development followed by Pliocene-Early Pleistocene aggradation was also interpreted for other locations in the lower part of Crna Reka basin, including Čulejca Cave, and attributed to the influence of the Messinian Salinity Crisis (Fig. 2; Temovski, 2016). The horizontal sections formed either during a stable base level in the same karst development phase as the shafts, or more likely during the development of Drenovo Gorge. In any case, the removal of the sediments was related to the incision by the Raec River through the Drenovo Gorge. The flowstone was deposited on top of an inclined sediment surface, and post-dates the time when the base level in the Drenovo Gorge was at a similar elevation as the cave. The subsequent incision in the Drenovo Gorge led to further removal of sediments below the flowstone deposits.

Table 2
Analytical data of the burial age determination in Temna Peštera – Dragožel.

Sample	Mass of quartz dissolved (g)	Mass of ^{9}Be carrier (g)	Natural Al content (ug/g $_{quartz}$)	Blk corrected ^{10}Be/^{9}Be (×10^{-14})	Blk corrected ^{26}Al/^{27}Al (×10^{-14})	^{10}Be (kat/gr$_{quartz}$)	^{26}Al (kat/gr$_{quartz}$)
TPD-01	28.9683	0.14186	370	5.16 ± 0.41	1.20 ± 0.17	37.90 ± 2.99	92.57 ± 15.31

Table 3
Simple burial age for the clastic sediment TPD-01 in Temna Peštera – Dragožel assuming complete burial and no redeposition (R0 = 6.8).

	Burial age (Ma)	Internal uncertainty* (Ma)	External uncertainty** (Ma)	Source denudation rate (m/ka)	External uncertainty (m/ka)
Complete burial (Granger and Muzikar, 2001)	2.08	0.38	0.49	–	–
Considering source and denudation rates, and all three types of cosmic ray particles (Braucher et al., 2011)	2.12	0.39	0.47	0.04	0.01

*Analytical uncertainties only; **analytical, half-lives and SLHL production rate of ^{10}Be and ^{26}Al/^{10}Be production rate ratio uncertainties.

Table 4
U-Th dating results of the speleothem samples.

Cave	Sample	Material	^{238}U (ppb)	^{232}Th (ppt)	^{230}Th/^{232}Th ($\times10^{-6}$)	δ^{234}U (‰)	^{230}Th/^{238}U	Age uncorr. (ka)	$\delta^{234}U_{in}$ (‰)	Age corr. (ka BP)
Liljarnikot	LJ1N	Flowstone	177.5 ± 0.3	39,931 ± 146	55.8 ± 0.4	8.8 ± 3.5	0.7612 ± 0.0056	153 ± 3	13 ± 5	146 ± 5
	LJ1-N2	Flowstone	188.8 ± 0.3	12,686 ± 28	164.0 ± 1.0	−12.1 ± 2.3	0.6681 ± 0.004	123 ± 1	−17 ± 3	121 ± 2
Temna Peštera – Dragožel	TPD-18-03-N1	Flowstone	285.3 ± 0.5	16,958 ± 52	317.1 ± 2.4	122.2 ± 5.5	1.1423 ± 0.008	418 ± 40	396 ± 48	416 ± 39
	TPD-18-03-N2	Flowstone	284.5 ± 0.4	5476 ± 51	989.6 ± 13.4	123.1 ± 2.7	1.1542 ± 0.0115	464 ± 70	455 ± 95	463 ± 69
	TPD-18-03-N3	Flowstone	413.1 ± 0.6	1047 ± 3	7557.4 ± 46.9	120.9 ± 2.7	1.1615 ± 0.0066	536 ± 80	549 ± 133	536 ± 80
	TPD-18-04-N1	Flowstone	215.5 ± 0.3	33,896 ± 401	133.9 ± 2.1	252.3 ± 3.9	1.275 ± 0.0137	336 ± 21	645 ± 39	333 ± 21
	TPD-18-04-N2	Flowstone	541.3 ± 0.8	12,222 ± 112	923.4 ± 12.5	173.8 ± 3	1.2638 ± 0.0128	/		
	TPD-18-04-N3	Flowstone	1058.9 ± 2.0	4710 ± 10	4189.2 ± 23	88.7 ± 3.4	1.1297 ± 0.0061	/		
Čulejca	CU4-A1	Mammillary calcite	97.8 ± 0.1	623 ± 2	2676.3 ± 12.1	28.5 ± 2.8	1.033 ± 0.004	543 ± 86	132 ± 37	543 ± 86
	CU4-A2	Mammillary calcite	81.4 ± 0.1	6339 ± 15	216.2 ± 1.1	42.7 ± 2.8	1.0205 ± 0.0047	365 ± 17	119 ± 10	363 ± 16
	CU4-N1	Mammillary calcite	101.2 ± 0.1	2509 ± 23	701.9 ± 9.4	37.3 ± 2.7	1.0549 ± 0.0105	/		
	CU4-N2	Mammillary calcite	48.0 ± 0.1	1930 ± 17	407.3 ± 5.3	29.8 ± 2.6	0.9928 ± 0.0094	338 ± 22	77 ± 8	336 ± 22
	CU4-NT	Mammillary calcite	125.8 ± 0.2	5324 ± 17	577.2 ± 3.1	259.2 ± 4.9	1.4806 ± 0.0068	/		
Podot	P2N-2	Mammillary calcite	421.9 ± 0.6	8384 ± 17	826.6 ± 3.6	94.3 ± 3.5	0.9957 ± 0.004	240 ± 5	185 ± 7	239 ± 5
	P2N-8	Mammillary calcite	342.6 ± 0.5	8475 ± 21	659.5 ± 4.3	109.3 ± 5.6	0.9893 ± 0.0061	222 ± 6	204 ± 11	222 ± 6
	P2N-9	Mammillary calcite	381.1 ± 0.6	869 ± 3	6723.2 ± 54.6	142.4 ± 4.1	0.9289 ± 0.0069	171 ± 3	231 ± 7	171 ± 3

5.2. Chronological constraints on Early to Middle Pleistocene cave and valley evolution

Deposition of clastic cave sediments and speleothems is largely controlled by the response of the karst systems to external geological, geomorphological and climatological forcings. While speleothem deposition corresponds to periods of suitable (wetter and warmer) climate conditions (e.g., Columbu et al., 2015), other factors (internal or external) can be of importance, depending on the speleothem depositional environment. This is particularly evident with subaqueous mammillary speleothems, that form close to the groundwater table (Hill and Forti, 1997). In karst aquifers draining large areas, subaqueous speleothem deposition can be continuous (albeit slow) even during severe climate conditions, that are reflected only in the speleothem geochemical record. However, as base-level lowering can cause lowering of the water table, subaqueous speleothem deposition at a particular location can cease. This allows mammillary speleothems to be used to reconstruct associated valley incision history, on the premise that the timing of water table lowering is coeval with the valley incision (e.g., Polyak et al., 2008).

An impressive paleoclimate record from the nearby Ohrid Lake (Figs. 1, 10; Wagner et al., 2019) allows us to compare the timing of speleothem and clastic cave sediment deposition in the study area to climate variations during the Pleistocene. In addition, this can help constrain the geomorphic significance of the geochronological data for the reconstruction of cave and valley evolution.

The flowstone plaque at Temna Peštera - Dragožel deposited between 416 ± 39 ka (TPD-18-03-N1) and 333 ± 21 ka (TPD-18-04-N1), and the studied mammillary section (CU4) at Čulejca between 363 ± 16 ka (CU4-A2) and 336 ± 22 ka (CU4-N2), the latter considered as a maximum age. The end of deposition is at a similar time for both samples, and coincides with the end of MIS 9e, a period generally characterized by a wetter climate terminating with an abrupt event of reduced precipitation according to the nearby Ohrid Lake record (Fig. 10; Regattieri et al., 2018; Wagner et al., 2019). The onset of deposition at CU4 is likely during MIS10, a prominent glacial, while onset of flowstone deposition at Temna Peštera – Dragožel is most likely during the MIS11 interglacial (Fig. 10).

The chronology of the cave deposits at Temna Peštera - Dragožel shows onset of deposition of clastic sediments as late as 2.12 ± 0.47 Ma, indicating that cave passage development commenced in the Early Pleistocene. As Temna Peštera - Dragožel development is also related to the development of Kamenica valley, following the draining of the Central Macedonian Lake (Temovski, 2016), the Early Pleistocene burial age of Temna Peštera - Dragožel agrees well with the Early Pleistocene (>1.6 Ma) draining of the lakes in Crna Reka drainage (Dumurdzanov

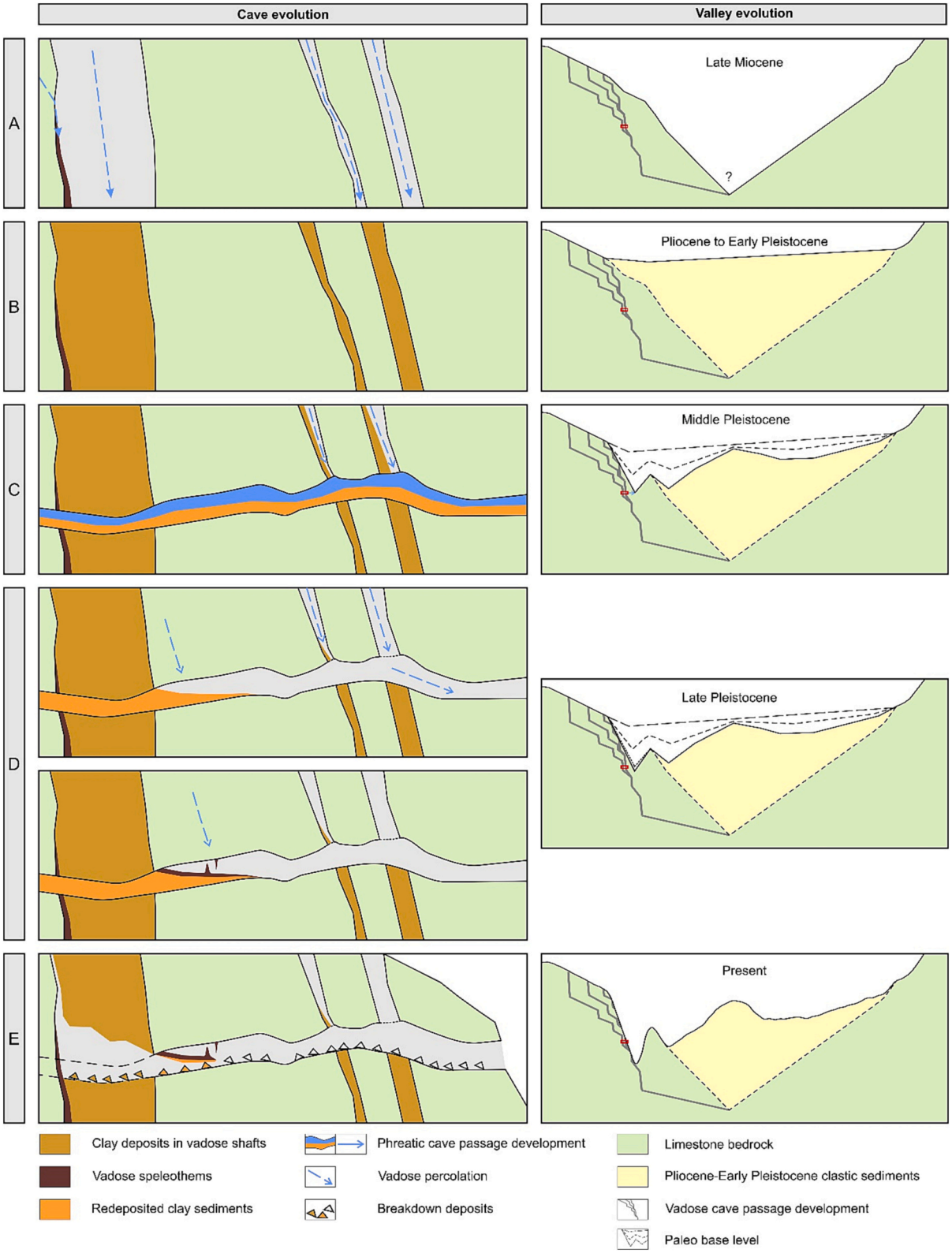

Fig. 9. Sketch of the interpreted speleogenetic phases of Liljarnikot Cave in relation to the valley evolution. A – Development of vadose shafts related to deep paleo-valley incision, with local deposition of flowstone, likely at the end of Late Miocene. B – Filling up of passages and closing of the karst system related to aggradation and base-level rise in the paleo-valley, likely during Pliocene-Early Pleistocene. C – Reactivation of the karst system after incision of the superimposed Drenovo Gorge following the draining of the Central Macedonian Lake in Middle Pleistocene, and subsequent development of sub-horizontal phreatic passages with redeposition of clastic sediments, related to stable base level likely during MIS 6. D – Partial removal of sediments by vadose waters and deposition of flowstone after lowering of base level in Late Pleistocene. E – Present situation after further removal of sediments and enlargement of the entrance by retreat of valley side related to the ongoing incision in the Drenovo Gorge.

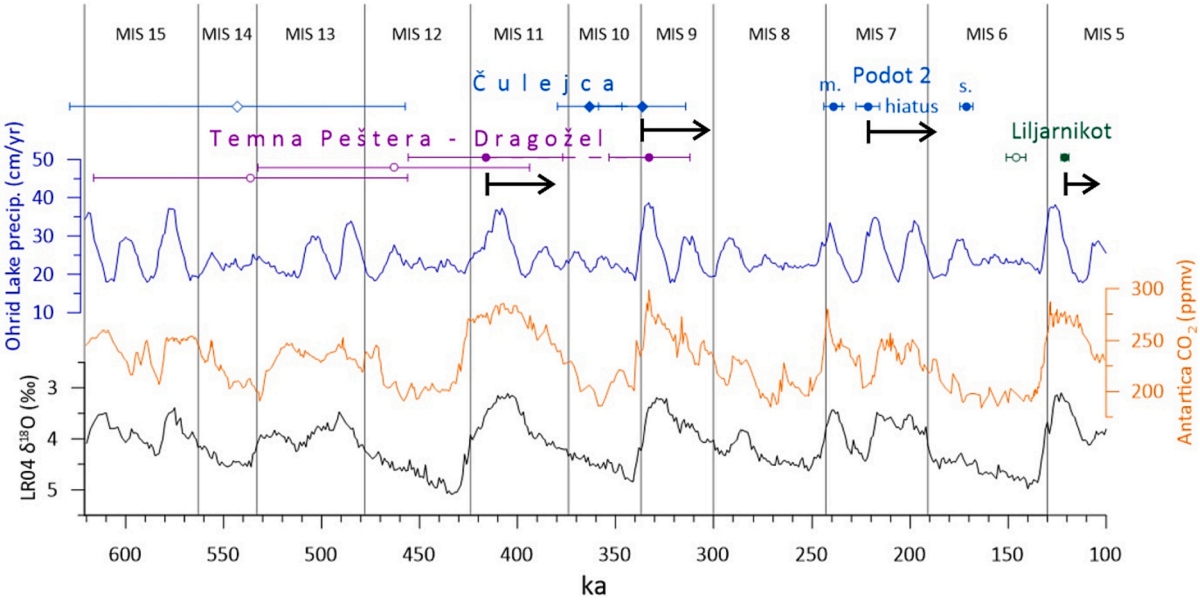

Fig. 10. Timing of speleothem formation in the studied caves of the Crna Reka drainage compared to Middle to Late Pleistocene climate changes as reflected in the benthic $\delta^{18}O$ record (LR04 stack; Lisiecki and Raymo, 2005), Antarctica ice core CO_2 record (composite of EPICA-Dome C and Vostok ice cores; Lüthi et al., 2008) and the simulated Ohrid Lake precipitation (Wagner et al., 2019). Open circles indicate outlier ages, excluded from interpretation. Black arrows indicate the interpreted base level lowering onset.

et al., 2005; Temovski et al., 2013). The minimum age for the clastic sediment deposition at Temna Peštera - Dragožel is constrained by the age of the base of the flowstone deposit (TPD-18-03-N1; 416 ± 39 ka), with last floods in the cave likely corresponding to the MIS 12 glacial period. Starting from MIS 11, the cave was already above the base level.

At Liljarnikot, the flowstone deposition follows either horizontal cave development between the clay-filled shafts with clay removal or just clay-removal from a previously existing horizontal passage, when the base level reached the cave. In both scenarios, the onset of flowstone deposition indicates draining of the cave, likely due to base-level lowering. Assuming that the ~121 ka age (LJ1-N2) is reliable, the flowstone might have formed during the Eemian (MIS 5e), with the last phreatic cave development phase occurring during the MIS 6 glacial.

The timing of the end of deposition at CU4 sample (CU4-N2; 336 ± 22 ka) is roughly coeval with a change to drier conditions (Fig. 10; Regattieri et al., 2018) suggesting a climate control on the deposition of the mammillary speleothem, that likely induced lowering of the water table. However, a lack of subsequent deposition at this location also indicates that this was coeval with, or followed by base-level lowering. This is also supported by the corrosion water level notch found below CU4 (Fig. 5). An alluvial notch that contains redeposited clay sediments is found at a similar elevation to this water-table notch, reflecting back-flooding from Crna Reka (Temovski, 2016). Therefore, the end of deposition at CU4 can be considered as the maximum age for the onset of base level lowering at the elevation of CU4.

The deposition of the P2 mammillary section at Podot Cave was during the MIS 7 (Fig. 10), and is related to the former position of Gugjakovo Springs (i.e., former water table). The large difference in age between the topmost part of the mammillary (222 ± 6 ka) and the spar (164 ± 2 ka) section indicates a depositional hiatus. The spar part grew during the MIS 6 glacial, probably in a restricted pool setting. Incision in Crna Reka in the later parts of MIS 7 likely lowered the spring position and terminated the mammillary speleothem deposition. This would explain why during the period of increased precipitation, as indicated by Ohrid Lake record (Fig. 10), there was no mammillary calcite deposition at this location. The subsequent spar calcite deposition during MIS 6 might be related to base-level rise due to aggradation in the Crna Reka riverbed, that allowed pool formation at this elevation, while the main spring was shifted laterally to a different position (probably towards the current one).

The obtained ages of the cave deposits are in agreement with the interpreted evolution of the studied caves and the conceptual model of the karst evolution in the area based on cave location, morphology and sediments (Temovski, 2016). Following the establishment of the lacustrine environments in Mariovo and Tikveš basins during the Pliocene (Dumurdzanov et al., 2004, 2005), the onset of draining of these lakes and subsequent valley incision in the Crna Reka drainage was as late as ~1.6 ± 0.05 Ma in the Buturica valley of the upstream Mariovo Basin (Temovski et al., 2013; Temovski, 2016), and ~2.1 ± 0.5 Ma in the Kamenica valley of the downstream Tikveš Basin (this study; Fig. 1). Subsequent lowering of the base level led to removal of basin sediments covering the karst terrains, incision of allogenic valley sections, and either reactivating fossilized karst systems (e.g., Čulejca Cave, Liljarnikot Cave) or developing new karst systems (e.g., karst on Vitačevo Plateau, Podot locality).

5.3. *Valley incision rates*

During constant tectonic uplift, the valley should incise to adjust its base to the uplift rate, thus the incision rate should equal the uplift rate (Bridgland and Westaway, 2008). However, climatic effects can greatly alter the base-level changes in a valley, with glacial periods generally contributing to base-level rises or lateral development (aggradation due to increase of sediment supply), and incision occurring during periods of climatic instability and transitions (e.g., Vandenberghe, 2003; Antoine et al., 2000; Bridgland and Westaway, 2008).

Based on the newly obtained chronological data, and the position of the studied caves above the current riverbed, cumulative valley incision rates were calculated (Fig. 11; Table 5). Depending on the type of the cave deposits, their position in the cave and relationship to the base level, the calculated cumulative incision rates represent minimum or maximum values.

Flowstone speleothems form in vadose conditions (Hill and Forti, 1997), after the lowering of the water table, and the timing of the onset of deposition marks the minimum age when the water table (i.e., base level) was at that position, thus they can provide maximum cumulative

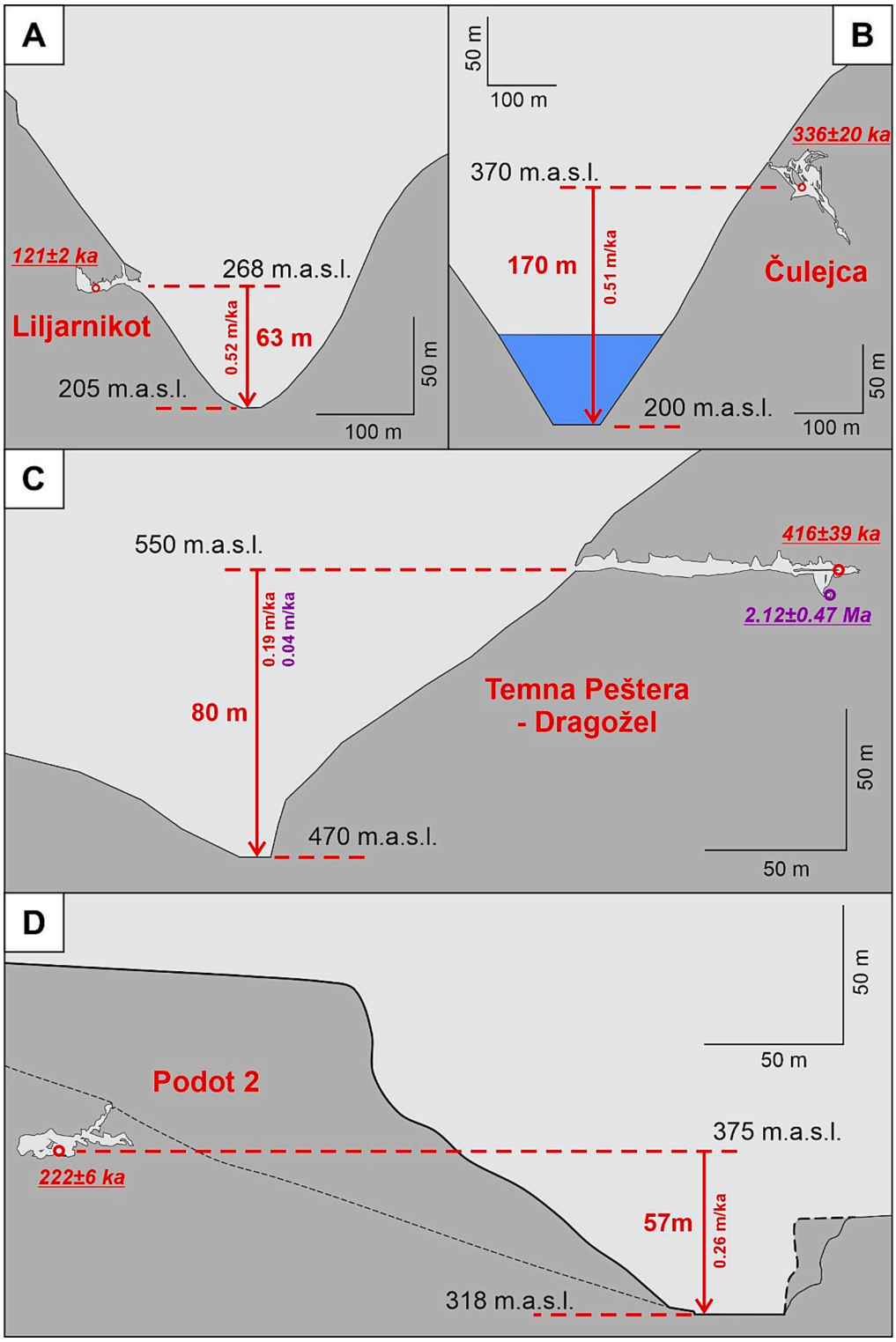

Fig. 11. Cross-sections of the studied caves showing their altitudinal relationship to the current river talweg and calculated valley incision rates based on the obtained geochronological data from the cave deposits. A – Liljarnikot Cave above Raec River. B – Čulejca Cave above Crna Reka. C – Temna Peštera – Dragožel above Kamenica River. D – Podot 2 Cave above Crna Reka. Circles indicate sample locations. For wider valley context see Fig. 3.

incision rates. At Temna Peštera – Dragožel, based on the age of onset of flowstone deposition, a maximum cumulative incision of 0.19 ± 0.2 m/ka in Kamenica valley was obtained for the last 416 ± 39 ka. Similarly, at Liljarnikot Cave, a maximum incision of 0.52 ± 0.01 m/ka of Raec River was calculated for the last 121 ± 2 ka (Table 5).

Subaqueous mammillary speleothems form close to the water table (Hill and Forti, 1997), and the timing of the end of speleothem deposition marks the maximum age when the water table (i.e., base level) was at that position, thus can provide a minimum cumulative incision rate. Based on the end of mammillary speleothem deposition at Čulejca Cave, a minimum incision rate of 0.51 ± 0.03 m/ka of Crna Reka valley was obtained for the last 336 ± 22 ka. Similarly, at Podot Cave, a minimum

Table 5
Valley incision and denudation rates in the Crna Reka drainage.

Valley	Cave/ location	Rel. elev. (m)	Dated material	Integration period/ time (ka)	Cumulative incision rate/ denudation rate (m/ka)
Raec	Liljarnikot	63	Flowstone	121 ± 2	0.52 ± 0.01*
Kamenica	Temna Peštera-Dragožel	80	Clastic sediment	2120 ± 470	0.04 ± 0.01**
Kamenica	Temna Peštera-Dragožel	80	Flowstone	416 ± 39	0.19 ± 0.02*
Kamenica	Budimirica[b]	80	Flowstone	83 ± 15	0.96 ± 0.17*
Crna Reka main valley	Čulejca	170	Mammillary speleothem	336 ± 20	0.51 ± 0.03**
Crna Reka main valley	Podot	57	Mammillary speleothem	222 ± 6	0.26 ± 0.01**
Buturica	Provalata[a]	90	Alunite	1600 ± 50	0.06 ± 0.002**
Blašnica	Allchar[c]	/	Quartz, dolomite/ calcite, sanidine, and diopside	<30	0.05–0.1***

Note that long-term incision rates and denudation rates are in good agreement with the temporal source denudation rate at ~2.1 Ma derived from the CRN data of the TPD-01 sample (Table 3).
[a] Based on Temovski et al. (2013).
[b] Temovski et al. (2013).
[c] Pavićević et al. (2016).
* Max cumulative rate.
** Min cumulative rate.
*** Temporal denudation rate.

incision rate of 0.26 ± 0.01 m/ka of Crna Reka valley was obtained for the last 222 ± 6 ka (Table 5).

A minimum cumulative incision rate is provided also based on the age of the clastic deposits, as they represent the maximum age when the base level was at that position. At Temna Peštera – Dragožel, based on the burial age of the sediment, the calculated long-term (2.12 ± 0.47 Ma) minimum cumulative incision rate is 0.04 ± 0.01 m/ka (Fig. 9; Table 5).

The calculated cumulative incision rates in the lower part of Crna Reka basin (Table 5) shows an increase towards the present (Fig. 12). The minimum incision rate of ~0.04 m/ka in Kamenica valley for the last ~2.1 Ma, inferred from the CRN burial age of the clastic cave sediments, is comparable to the incision rate of 0.06 m/ka (Table 5) in the middle part of Buturica valley for the last 1.6 Ma, based on Ar-Ar dating of alunite minerals in Provalata Cave (Figs. 12, 13), that reflects former water-table sulfuric acid speleogenesis (Temovski et al., 2013). These values are also in good agreement with the CRN-based temporal denudation rates from the region: the long-term recent (<30 ka) denudation rates of 0.05–0.1 m/ka at the Allchar ore in the upstream part of Blašnica valley (Figs. 12, 13, Table 5; Pavićević et al., 2016), as well as the paleo (~2.1 Ma) denudation rate of ~0.04 m/ka derived from the buried sediment in Temna Peštera – Dragožel (this study). For the Middle to Late Pleistocene, where the time constraints are provided by the U-Th dated speleothems, the inferred incision rates appear to be independent from the dated speleothem type. Thus, regardless of whether they reflect minimum or maximum cumulative incision rates, they show an increase in the Middle Pleistocene (from ~0.2 to 0.5 m/ka), to even higher values in the Late Pleistocene (up to 1 m/ka) (Table 5, Fig. 12).

The estimated incision rates as well as their increasing trend towards present are in agreement with published incision/uplift rates throughout Europe (Fig. 10 in Ruszkiczay-Rüdiger et al., 2020). Similar values and trends have also been found in the Dinarides-Hellenides. For example, in the central and southern parts of Albania, incision rates range from ~0.4 to ~1.5 m/ka for the Last Pleistocene, with even higher values found in more recent times, and with an increase towards the hinterland (Carcaillet et al., 2009). In the NE Peloponnese (Greece), incision rates of 0.1

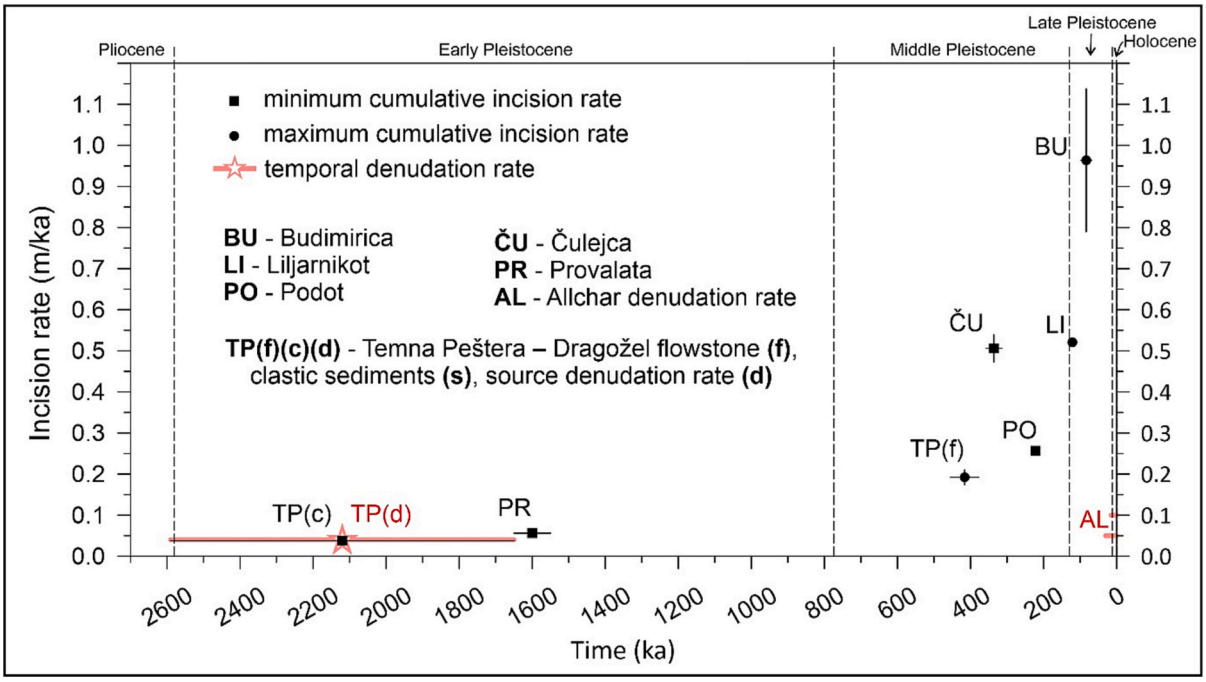

Fig. 12. Relationship of valley incision rates and time in the lower part of Crna Reka basin. The x-axis represents the integration time interval until present for the estimated cumulative incision rates (given as minimum or maximum values). The denudation rates are temporal rates, representative only for the specific time period indicated, with the star symbol for TP(d) indicating the most probable age.

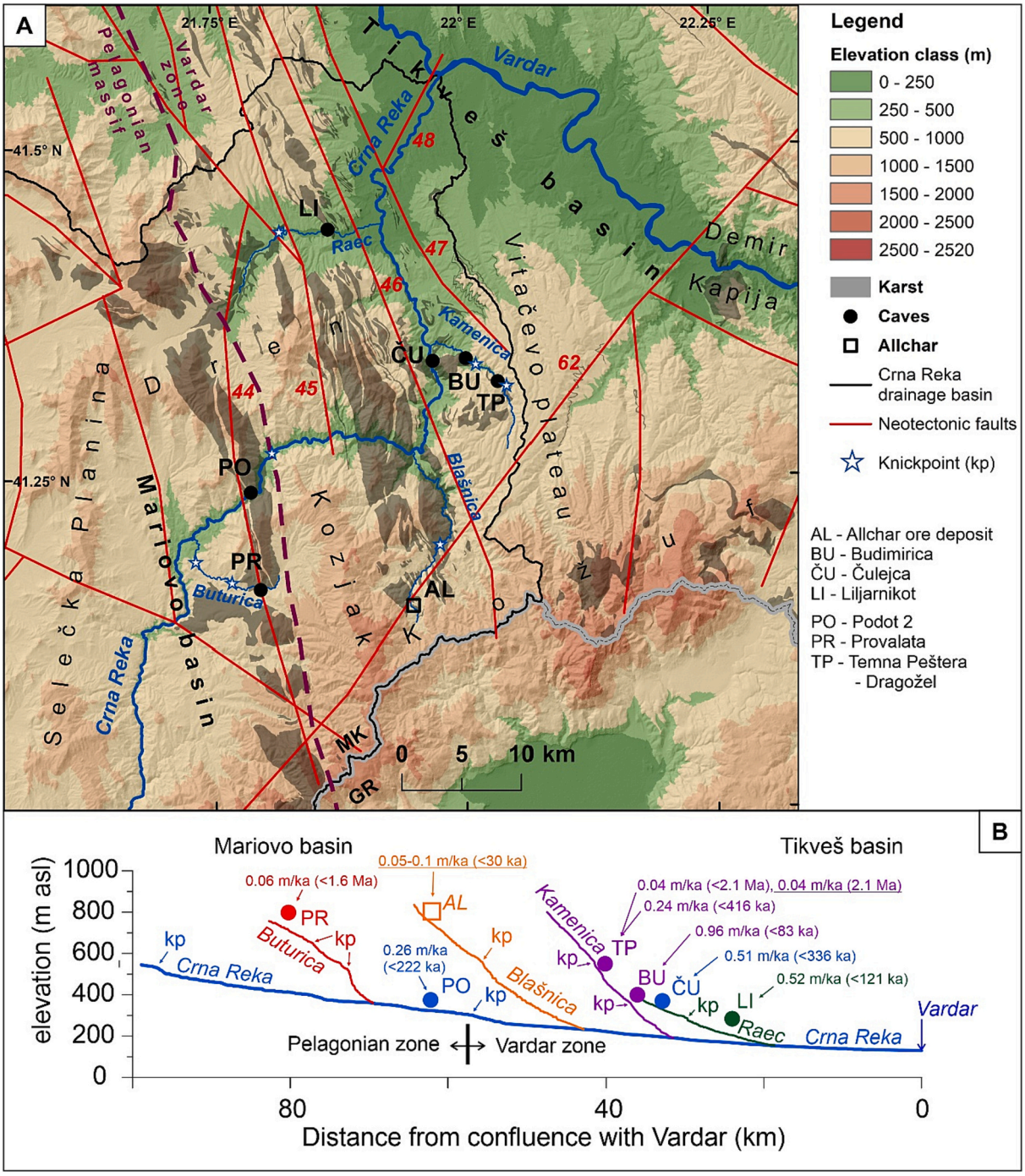

Fig. 13. River drainage in the lower part of Crna Reka basin. A – location of the sites with estimated valley incision rates. Neotectonic faults are from Arsovski (1997). Weakly seismogenic faults are marked with numbers: 44 – Dudičk–, 45 - Klepsk–, 46 - Mrežičk–, 47 - Svekjansk–, 48 - Stobiski, 62 – Vitačevsko-Demirkapiski. B – Longitudinal profiles of Crna Reka and its tributaries in the study area, with the locations of the sites with estimated cumulative incision rates. Underlined values represent temporal denudation rates. Coloring reflects corresponding valleys.

to 1.3 m/ka for the last 580 ka were found, with values increasing at locations close to a major active fault along the southern edge of the Corinth Rift (Karymbalis et al., 2016). However, it is difficult to have a more direct comparison to the incision rates obtained from Crna Reka drainage, as they belong to different drainage systems, and can reflect also regional geological and tectonic variations, as well as different expression of the climatic control.

5.4. *Insight into regional tectonic uplift*

Similar timing of the onset of the draining of the paleolakes in the upstream (1.60 ± 0.05 Ma; Temovski et al., 2013) and downstream (2.12 ± 0.47 Ma; this study) part of the Crna Reka drainage in the Early Pleistocene, as indicated by cave geochronology, suggests that regional uplift was the more likely cause for the draining of these lakes, rather than headward erosion from Vardar River related to subsidence in the Aegean Sea (e.g., Dumurdzanov et al., 2005).

The much higher cumulative incision rates since the Middle

Pleistocene might reflect an increase in the uplift rates in the region, or can reflect the transition in the Earth climate cyclicity since Middle Pleistocene (Gibbard and Lewin, 2009). However, such negative power-law relationships between cumulative incision rates and integrating time have been found to indicate climate-triggered non-steady state behavior in valley incision, instead of an increase in tectonic uplift rates (Finnegan et al., 2014; Ruszkiczay-Rüdiger et al., 2020; Zondervan et al., 2022). This widely observed apparent acceleration of river incision towards the present is mostly likely a result of the averaging of incision rates over longer times, that will include also periods of no incision such as during glacial periods where increase in sediment supply can lead to lateral planation or aggradation (Hancock and Anderson, 2002). However, on the shorter timescales, the most recent fluvial response is commonly downcutting, associated with the decreased sediment input since the Last Glacial Maximum. This apparent increase is commonly observed in river systems in Europe and worldwide, and should not be mistaken for a real increase in tectonic uplift rates (Finnegan et al., 2014; Ruszkiczay-Rüdiger et al., 2020).

The differences in the cumulative incision rates in the study area can reflect differential tectonic uplift and/or an external base level control, i.e., headward erosion. For example, knickpoint retreat initiated by external base-level changes (e.g., in the main Vardar River valley) could cause differences in the incision rates between downstream and upstream parts of a valley system (e.g., Rixhon et al., 2011). Such differences are observable in each of the tributary valleys, including the main Crna Reka valley, with notable knickpoints present downstream from the sections with lower incision rates (Fig. 13). Such an effect is probably at least partly attributable to the lowest incision rates found in the upstream parts of Buturica and Blašnica valleys (Fig. 13).

However, headward erosion cannot explain the higher incision rate found at Čulejca (0.51 m/ka) in its downstream part, compared to the incision rate at Podot (0.26 m/ka) located further upstream in the Crna Reka valley. Although both of these values are minimum cumulative incision rates, considering that the value at Čulejca integrates a longer period (<336 ka) than Podot (<222 ka), if the uplift rate is the same, this should lead to the opposite, i.e., Podot having higher incision rate than Čulejca. Thus, this implies higher uplift rates occurred at Čulejca, in the NW part of Vitačevo plateau. The highest calculated incision rates (0.96 ± 0.17 m/ka) were also found in this area, at Budimirica Cave in the Kamenica valley (Table 5, Fig. 13; Temovski et al., 2016). This value represents a maximum cumulative incision rate, therefore the river incision rate at the NW part of the Vitačevo plateau appears to be bracketed between ~0.96 m/ka and ~0.51 m/ka (minimum average incision rate at Čulejca), integrated over ~83 ka and ~336 ka, respectively. This area is bounded by seismogenic faults, with registered earthquakes with magnitudes of 5.5 and 5.3 ML along the Mrežički and Vitačevsko-Demirkapiski faults (Fig. 13; Arsovski, 1997; Drogreška, 2018), that might explain the higher calculated incision rates. The much smaller values at Temna Peštera – Dragožel (0.19 m/ka, integrated for ~416 ka) located further upstream in Kamenica valley might be partly due to a knickpoint located in-between the two locations (Fig. 13). A strong erosion evidenced in the Budimirica Cave sediments was attributed to migration of this knickpoint upstream from Budimirica Cave during MIS 3 – MIS 2 (Temovski et al., 2016).

Tectonic uplift rates of 1.1–1.2 m/ka were measured by geodetic leveling in the lower part of Crna Reka drainage for the period 1935–1958 (Lilienberg, 1968). These uplift rates are comparable to the cumulative incision rates based on the newly obtained geochronological data for the same area (Liljarnikot, Čulejca, Budimirica), with a maximum value of 0.96 ± 0.17 m/ka integrated over the shortest period of 83 ± 15 ka, suggesting significant tectonic control on the valley incision in the area. The tectonic activity in the area is also supported by the recent GPS measurements that show southward horizontal movement of the crust in Macedonia, with southernmost sections consistent with recent N-S extension in N. Macedonia and Greece (Burchfiel et al., 2006). It should be noted that these uplift rates might somewhat overestimate the real uplift in the area, considering that the highest cumulative incision rates obtained integrate the period of fast incision during the last glacial-interglacial transition, and the rates relevant for longer periods of time are even lower. However, similar incision rates (~0.5 m/ka for the last 77 ka) were found also at Menikio Mt. in NE Greece (Pennos et al., 2019), and these values are within range of GPS-based vertical deformation rates in the Hellenides (0.5–1.0 m/ka; Serpelloni et al., 2022).

6. Conclusion

Age determination of cave deposits was successfully applied to constrain the timing of cave evolution in the drainage of the Crna Reka river in the central parts of the Balkan Peninsula, and to quantify minimum and maximum rates of base-level lowering, a relevant measure of river incision rate in the study area.

Cosmogenic nuclide burial age dating of clastic sediments, applied for the first time in this region, shows that Temna Peštera – Dragožel Cave was already active in the Early Pleistocene (2.1 ± 0.5 Ma). This confirms that removal of sediments covering the karst rocks in the Vitačevo Plateau was already initiated in the Early Pleistocene. That places the onset of draining of the Central Macedonian Lake in the Early Pleistocene as well, in general agreement with the understanding of the evolution of Tikveš basin. Furthermore, the similar timing of the onset of the draining in the upstream and downstream parts of the Crna Reka drainage suggest that this was more likely initiated by regional uplift, rather than headward erosion related to subsidence in the Aegean Sea. The Middle to Late Pleistocene age of the speleothems from the caves in the lower part of the Crna Reka drainage was determined by U-Th dating, in agreement with the conceptual model for karst evolution in this region.

Calculated cumulative valley incision rates based on the obtained radiometric data show an increase towards the present, with values of <0.1 m/ka in the Early Pleistocene, increasing to ~0.2–0.5 m/ka in the Middle Pleistocene, and up to 1 m/ka in the Late Pleistocene. The apparent acceleration of incision rates integrated over shorter time might be a result of integrating the fast incision triggered by the last glacial-interglacial transition. Higher Middle to Late Pleistocene uplift is inferred for the downstream part of Crna Reka (e.g., NW part of Vitačevo plateau), an area in the Vardar zone bounded by seismogenic faults, with respect to the upstream part, at the easternmost edge of the Pelagonian massif. The estimated maximum cumulative incision rates for the downstream part of Crna Reka drainage of ~0.96 m/ka (representative for the last ~83 ka) are similar to the recently measured uplift rates in the area (1.1–1.2 m/ka), and overlap with the range of GPS-based vertical deformation rates in the Hellenides (0.5–1 m/ka).

CRediT authorship contribution statement

Marjan Temovski: Conceptualization, Formal analysis, Investigation, Methodology, Resources, Validation, Visualization, Writing – original draft, Writing – review & editing. **Alexander Wieser:** Methodology, Writing – review & editing, Validation. **Oscar Marchhart:** Methodology, Writing – review & editing, Validation. **Mihály Braun:** Methodology. **Balázs Madarász:** Investigation, Writing – review & editing. **Gabriella Ilona Kiss:** Methodology, Validation, Writing – review & editing. **László Palcsu:** Funding acquisition, Methodology, Resources, Validation, Writing – review & editing, Project administration. **Zsófia Ruszkiczay-Rüdiger:** Formal analysis, Funding acquisition, Investigation, Methodology, Project administration, Resources, Validation, Writing – review & editing.

Declaration of competing interest

The authors declare that they have no known competing financial interests or personal relationships that could have appeared to influence

the work reported in this paper.

Data availability

Data will be made available on request.

Acknowledgments

This research was supported by the National Research, Development and Innovation Office of Hungary grant OTKA FK 124807 and by the European Union and the State of Hungary, co-financed by the European Regional Development Fund in the project of GINOP-2.3.2-15-2016-00009 'ICER'. AMS measurements at Vienna Environmental Research Accelerator, were supported by the RADIATE Transnational Access grant 22002703-ST. Fieldwork was carried out under Research Permits Nos. UP1-11/1-770/2017, UP1-11/1-423/2018, UP1-11/1-1755/2018 and UP1-11/1-1830/2019 issued to SK Zlatovrv Prilep by the Ministry of Environment and Physical Planning of the Republic of Macedonia. We thank Zlatko Angeleski, Darko Nedanoski and other cavers from SK Zlatovrv Prilep for assistance during fieldwork. We are also thankful to Jo De Waele and two anonymous reviewers, as well as the Editor Martin Stokes, for their useful comments and suggestions that improved the manuscript.

References

Akhmadaliev, S., Heller, R., Hanf, D., Rugel, G., Merchel, S., 2013. The new 6 MV AMS facility DREAMS at Dresden. Nucl. Instrum. Methods B 294, 5–10. https://doi.org/10.1016/j.nimb.2012.01.053.

Antoine, P., Lautridou, J.P., Laurent, M., 2000. Long-term fluvial archives in NW France: response of the Seine and Somme rivers to tectonic movements, climatic variations and sea-level changes. Geomorphology 33, 183–207. https://doi.org/10.1016/S0169-555X(99)00122-1.

Arsovski, M., 1997. Tektonika na Makedonija. Rudarsko-geološki fakultet, Štip (in Macedonian).

Balco, G., 2017. Production rate calculations for cosmic-ray-muon-produced 10Be and 26Al benchmarked against geological calibration data. Quat. Geochronol. 39, 150–173. https://doi.org/10.1016/j.quageo.2017.02.001.

Bella, P., Bosák, P., Braucher, R., Pruner, P., Hercman, H., Minár, J., Veselský, M., Holec, J., Léanni, L., 2019. Multi-level Domica–Baradla cave system (Slovakia, Hungary): Middle Pliocene–Pleistocene evolution and implications for the denudation chronology of the Western Carpathians. Geomorphology 327, 62–79. https://doi.org/10.1016/j.geomorph.2018.10.002.

Borchers, B., Marrero, S.M., Balco, G., Caffee, M.W., Goehring, B.M., Lifton, N.A., Nishiizumi, K., Phillips, F.M., Schaefer, J.M., Stone, J.O., 2016. Geological calibration of spallation production rates in the CRONUS-Earth project. Quat. Geochronol. 31, 188–198. https://doi.org/10.1016/j.quageo.2015.01.009.

Braucher, R., Merchel, S., Borgomano, J., Bourles, D.L., 2011. Production of cosmogenic radionuclides at great depth: a multi element approach. Earth Planet. Sci. Lett. 309, 1–9. https://doi.org/10.1016/j.epsl.2011.06.036.

Bridgland, D.R., Westaway, R., 2008. Climatically controlled river terrace staircases: a worldwide Quaternary phenomenon. Geomorphology 98, 285–315. https://doi.org/10.1016/j.geomorph.2006.12.032.

Budaj, M., Mudrak, S., 2008. Therion—digital cave maps. In: Proceedings of the IV European Speleological Congress, Lans-en-Vercors, France, 33. Spelunca Memoires, pp. 138–141.

Burchfiel, B.C., King, R.W., Todosov, A., Kotzev, V., Durmurdzanov, N., Serafimovski, T., Nurce, B., 2006. GPS results for Macedonia and its importance for the tectonics of the Southern Balkan extensional regime. Tectonophysics 413, 239–248. https://doi.org/10.1016/j.tecto.2005.10.046.

Burchfiel, B.C., Nakov, R., Dumurdzanov, N., Papanikolaou, D., Tzankov, T., Serafimovski, T., King, R.W., Kotzev, V., Todosov, A., Nurce, B., 2008. Evolution and dynamics of the Cenozoic tectonics of the South Balkan extensional system. Geosphere 4, 919–938. https://doi.org/10.1130/GES00169.1.

Carcaillet, J., Mugnier, J.L., Koçi, R., Jouanne, F., 2009. Uplift and active tectonics of southern Albania inferred from incision of alluvial terraces. Quat. Res. 71, 465–476. https://doi.org/10.1016/j.yqres.2009.01.002.

Cheng, H., Edwards, R.L., Shen, C.-C., Polyak, V.J., Asmerom, Y., Woodhead, J., Hellstrom, J., Wang, Y.J., Kong, X., Spötl, C., Wang, X.F., Alexander Jr., E.C., 2013. Improvements in 230Th dating, 230Th and 234U half-life values, and U–Th isotopic measurements by multi-collector inductively coupled plasma mass spectrometry. Earth Planet. Sci. Lett. 371–372, 82–91. https://doi.org/10.1016/j.epsl.2013.04.006.

Chmeleff, J., von Blanckenburg, F., Kossert, K., Jakob, D., 2010. Determination of the 10Be half-life by multicollector ICP-MS and liquid scintillation counting. Nuclear Instruments & Methods in Physics Research, Section B, Beam Interactions with Materials and Atoms 268, 192–199. https://doi.org/10.1016/j.nimb.2009.09.012.

Clauzon, G., Suc, J.-P., Dumurdžanov, N., Melinte-Dobrinescu, M., Zagorchev, I., 2008. The Pliocene Gilbert-type fan delta of Dračevo (Skopje area, Republic of Macedonia). Geol. Maced. 2, 21–28.

Columbu, A., De Waele, J., Forti, P., Montagna, P., Picotti, V., Pons-Branchu, E., Hellstrom, J., Bajo, P., Drysdale, R., 2015. Gypsum caves as indicators of climate-driven river incision and aggradation in a rapidly uplifting region. Geology 43 (6), 539–542. https://doi.org/10.1130/G36595.1.

Columbu, A., Audra, P., Gázquez, F., D'Angeli, I.M., Bigot, J.Y., Koltai, G., Chiesa, R., Yu, T.-L., Hu, H.-M., Shen, C.-C., Carbone, C., Heresanu, V., Nobécourt, J.-C., De Waele, J., 2021. Hypogenic speleogenesis, late stage epigenic overprinting and condensation-corrosion in a complex cave system in relation to landscape evolution (Toirano, Liguria, Italy). Geomorphology 376, 107561. https://doi.org/10.1016/j.geomorph.2020.107561.

De Waele, J., Gutiérrez, F., 2022. Karst Hydrogeology, Geomorphology and Caves, First edition. John Wiley & Sons. https://doi.org/10.1002/9781119605379.

Dorale, J.A., Edwards, R.L., Alexander, E.C., Shen, C.-C., Richards, D.A., Cheng, H., 2007. Uranium-series dating of speleothems: current techniques, limits, and applications. In: Sasowsky, I.D., Mylroie, J.R. (Eds.), Studies of Cave Sediments. Springer, Dordrecht, pp. 177–197. https://doi.org/10.1007/978-1-4020-5766-3_10.

Drogreška, K., 2018. Use of the Dislocation Theory in Defining the Epicentral Areas and Tectonic Conditions in the Territory of the Republic of Macedonia. Ss. Cyril and Methodius University, Skopje (PhD thesis.).

Dumurdzanov, N., Serafimovski, T., Burchfiel, B.C., 2004. Evolution of the Neogene-Pleistocene basins of Macedonia. In: Geol Soc Am Digit Map Chart Ser, 1, pp. 1–20. https://doi.org/10.1130/2004-dumurdzanov-macedonia.

Dumurdzanov, N., Serafimovski, T., Burchfiel, B.C., 2005. Cenozoic tectonics of Macedonia and its relation to the South Balkan extensional regime. Geosphere 1, 1–22. https://doi.org/10.1130/GES00006.1.

Edwards, R.L., Chen, J.H., Wasserburg, G.J., 1987. 238U, 234U, 230Th, 232Th systematics and the precise measurement of time over the past 500,000 years. Earth Planet. Sci. Lett. 81, 175–192. https://doi.org/10.1016/0012-821X(87)90154-3.

Fenton, C.R., Binnie, S.A., Dunai, T., Niedermann, S., 2022. The SPICE project: Calibrated cosmogenic 26Al production rates and cross-calibrated 26Al/10Be, 26Al/14C, and 26Al/21Ne ratios in quartz from the SP basalt flow, AZ, USA. Quat. Geochronol. 67, 101218 https://doi.org/10.1016/j.quageo.2021.101218.

Finnegan, N.J., Schumer, R., Finnegan, S., 2014. A signature of transience in bedrock river incision rates over timescales of 10^4–10^7 years. Nature 505, 391–396. https://doi.org/10.1038/nature12913.

Ford, D., Williams, P., 2007. Karst Hydrogeology and Geomorphology, 2nd ed. Wiley, Chichester.

Genuite, K., Voinchet, P., Delannoy, J.-J., Bahain, J.-J., Monney, J., Arnaud, J., Bruxelles, L., Moncel, M.-H., Philippe, A., Pons-Branchu, E., Revil, A., Richard, M., Jaillet, S., 2022. Middle and Late Pleistocene evolution of the Ardèche Valley archaeological landscapes (France). Quat. Sci. Rev. 297, 107812 https://doi.org/10.1016/j.quascirev.2022.107812.

Gibbard, P.L., Lewin, J., 2009. River incision and terrace formation in the Late Cenozoic of Europe. Tectonophysics 474, 41–55. https://doi.org/10.1016/j.tecto.2008.11.017.

Gosse, J.C., Phillips, F.M., 2001. Terrestrial cosmogenic nuclides: theory and applications. Quat. Sci. Rev. 20, 1475–1560. https://doi.org/10.1016/S0277-3791(00)00171-2.

Granger, D.E., 2006. A review of burial dating methods using 26Al and 10Be. Geol. Soc. Am. Spec. Pap. 415, 1–16. https://doi.org/10.1130/2006.2415(01).

Granger, D.E., 2014. Cosmogenic nuclide burial dating in archaeology and paleoanthropology. In: Holland, H.D., Turekian, K.K. (Eds.), Treatise on Geochemistry, , second edition14. Elsevier, Oxford, pp. 81–97. https://doi.org/10.1016/B978-0-08-095975-7.01208-0.

Granger, D.E., Muzikar, P.F., 2001. Dating sediment burial with in situ-produced cosmogenic nuclides: theory, techniques, and limitations. Earth Planet. Sci. Lett. 188, 269–281. https://doi.org/10.1016/S0012-821X(01)00309-0.

Granger, D.E., Fabel, D., Palmer, A.N., 2001. Pliocene-Pleistocene incision of the Green River, Kentucky, determined from radioactive decay of cosmogenic 26Al and 10Be in Mammoth Cave sediments. GSA Bull. 113 (7), 825–836 doi:10.1130/0016-7606(2001)113%3C0825:PPIOTG%3E2.0.CO;2.

Hancock, G.S., Anderson, R.S., 2002. Numerical modeling of fluvial strath-terrace formation in response to oscillating climate. Geol. Soc. Am. Bull. 114, 1131–1142 doi:10.1130/0016-7606(2002)114%3C1131:NMOFST%3E2.0.CO;2.

Harmand, D., Adamson, K., Rixhon, G., Jaillet, S., Losson, B., Devos, A., Hez, G., Calvet, M., Audra, P., 2017. Relationships between fluvial evolution and karstification related to climatic, tectonic and eustatic forcing in temperate regions. Quat. Sci. Rev. 166, 38–56. https://doi.org/10.1016/j.quascirev.2017.02.016.

Häuselmann, Ph., Granger, D.E., Lauritzen, S.-E., Jeannin, P.-Y., 2007. Abrupt glacial valley incision at 0.8 Ma dated from cave deposits in Switzerland. Geology 35, 143–146. https://doi.org/10.1130/G23094A.

Häuselmann, P., Mihevc, A., Pruner, P., Horáček, I., Čermák, S., Hercman, H., Sahy, D., Fiebig, M., Zupan Hajna, N., Bosák, P., 2015. Snežna jama (Slovenia): interdisciplinary dating of cave sediments and implication for landscape evolution. Geomorphology 247, 10–24. https://doi.org/10.1016/j.geomorph.2014.12.034.

Heisinger, B., Lal, D., Jull, A.J., Kubik, P.W., Ivy-Ochs, S., Neumaier, S., Knie, K., Lazarev, V., Nolte, E., 2002a. Production of selected cosmogenic radionuclides by muons 1. Fast muons. Earth Planet. Sci. Lett. 200, 345–355. https://doi.org/10.1016/S0012-821X(02)00640-4.

Heisinger, B., Lal, D., Jull, A.J., Kubik, P., Ivy-Ochs, S., Knie, K., Nolte, E., 2002b. Production of selected cosmogenic radionuclides by muons: 2. Capture of negative muons. Earth Planet. Sci. Lett. 200, 357–369. https://doi.org/10.1016/S0012-821X(02)00641-6.

Hill, C.A., Forti, P., 1997. Cave Minerals of the World. National Speleological Society, Huntsville, AL.
Hill, C.A., Polyak, V.J., 2020. A karst hydrology model for the geomorphic evolution of Grand Canyon, Arizona, USA. Earth Sci. Rev. 208, 103279 https://doi.org/10.1016/j.earscirev.2020.103279.
Jaffey, A.H., Flynn, K.F., Glendenin, L.E., Bentley, W.C., Essling, A.M., 1971. Precision measurement of half-lives and specific activities of 235U and 238U. Phys. Rev. C4, 1889–1906.
Karymbalis, E., Papanastassiou, D., Gaki-Papanastassiou, K., Ferentinou, M., Chalkias, C., 2016. Late Quaternary rates of stream incision in Northeast Peloponnese, Greece. Front. Earth Sci. 10 (3), 455–478. https://doi.org/10.1007/s11707-016-0577-0.
Kaufman, A., Broecker, W.S., 1965. Comparison of 230Th and 14C ages for carbonate materials from lakes Lahontan and Bonneville. J. Geophys. Res. 70, 4039. https://doi.org/10.1029/JZ070i016p04039.
Kolčakovski, D., Milevski, I., 2012. Recent landform evolution in Macedonia. In: Loczy, D., Stankoviansky, M., Kotarba, A. (Eds.), Recent Landform Evolution. The Carpatho-Balkan-Dinaric Region. Springer, pp. 413–442. https://doi.org/10.1007/978-94-007-2448-8_15.
Korschinek, G., Bergmaier, A., Faestermann, T., Gerstmann, U.C., Knie, K., Rugel, G., Wallner, A., Dillmann, I., Dollinger, G., Lierse von Gostomski, Ch., Kossert, K., Maiti, M., Poutivtsev, M., Remmert, A., 2010. A new value for the half-life of 10Be by heavy-ion elastic recoil detection and liquid scintillation counting. Nucl. Instrum. Methods Phys. Res., Sect. B 268, 187–191. https://doi.org/10.1016/j.nimb.2009.09.020.
Lachner, J., Martschini, M., Kalb, A., Kern, M., Marchhart, O., Plasser, F., Priller, A., Steier, P., Wieser, A., Golser, R., 2021. Highly sensitive 26Al measurements by ion-laser-interaction mass spectrometry. Int. J. Mass Spectrom. 465, 116576 https://doi.org/10.1016/j.ijms.2021.116576.
Lal, D., 1991. Cosmic ray labeling of erosion surfaces – in situ nuclide production rates and erosion models. Earth Planet. Sci. Lett. 104 (2–4), 424–439. https://doi.org/10.1016/0012-821X(91)90220-C.
Lilienberg, D.A., 1968. The main regularities in recent movements in the central parts of the Balkan peninsula (on the example of Macedonia). Stud. Geophys. Geod. 12, 163–178. https://doi.org/10.1007/BF02587845.
Lisiecki, L.E., Raymo, M.E., 2005. A Pliocene-Pleistocene stack of 57 globally distributed benthic d18O records. Paleoceanography 20, PA1003. https://doi.org/10.1029/2004PA001071.
Lüthi, D., Le Floch, M., Bereiter, B., Blunier, T., Barnola, J.-M., Siegenthaler, U., Raynaud, D., Jouzel, J., Fischer, H., Kawamura, K., Stocker, T.F., 2008. High-resolution carbon dioxide concentration record 650,000-800,000 years before present. Nature 453, 379–382. https://doi.org/10.1038/nature06949.
Manakovik, D., Andonovski, T., 1984. Geomorfologija. In: Mariovo - kopleksni geografski proučuvanja. Geografski fakultet, Skopje, pp. 41–81 (in Macedonian).
Manakovik, D., Andonovski, T., Stojanovik, M., Stojmilov, A., 1998. Geomorphological map of the Republic of Macedonia. Geogr. Rev. 32–33, 37–70 (in Macedonian).
Merchel, S., Herpers, U., 1999. An update on radiochemical separation techniques for the determination of long-lived radionuclides via accelerator mass spectrometry. Radiochim. Acta 84, 215–219. https://doi.org/10.1524/ract.1999.84.4.215.
Merchel, S., Bremser, W., Bourles, D.L., Czeslik, U., Erzinger, J., Kummer, N.A., Leanni, L., Merkel, B., Recknagel, S., Schaefer, U., 2013. Accuracy of 9 Be-data and its influence on 10 Be cosmogenic nuclide data. J. Radioanal. Nucl. Chem. 298 (3), 1871–1878. https://doi.org/10.1007/s10967-013-2746-x.
Merchel, S., Gärtner, A., Beutner, S., Bookhagen, B., Chabilan, A., 2019. Attempts to understand potential deficiencies in chemical procedures for AMS: cleaning and dissolving quartz for 10Be and 26Al analysis. Nucl. Inst. Methods Phys. Res. B 455, 293–299. https://doi.org/10.1016/j.nimb.2019.02.007.
Milevski, I., 2015. General geomorphological characteristics of the Republic of Macedonia. Geogr. Rev. 48, 5–25.
Nishiizumi, K., 2004. Preparation of 26Al AMS standards. Nucl. Instrum. Methods Phys. Res., Sect. B 223–224, 388–392. https://doi.org/10.1016/j.nimb.2004.04.075.
Nørgaard, J., Jansen, J.D., Neuhuber, S., Ruszkiczay-Rüdiger, Z., Knudsen, M.F., 2023. P–PINI: a cosmogenic nuclide burial dating method for landscapes undergoing non-steady erosion. Quat. Geochronol. 74, 101420 https://doi.org/10.1016/j.quageo.2022.101420.
Palmer, A.N., 2007. Cave Geology. Cave Books, Dayton, Ohio.
Pavićević, M.K., Cvetković, V., Niedermann, S., Pejović, V., Amthauer, G., Boev, B., Bosch, F., Aničin, I., Henning, W.F., 2016. Erosion rate study at the Allchar deposit (Macedonia) based on radioactive and stable cosmogenic nuclides (26Al, 36Cl, 3He, and 21Ne). Geochem. Geophys. Geosyst. 17, 410–424. https://doi.org/10.1002/2015GC006054.
Pennos, C., Lauritzen, S.E., Vouvalidis, K., Cowie, P., Pechlivanidou, S., Gkarlaouni, C., Styllas, M., Tsourlos, P., Mouratidis, A., 2019. From subsurface to surface: a multidisciplinary approach to decoding uplift histories in tectonically-active karst landscapes. Earth Surf. Process. Landf. 44, 1710–1721. https://doi.org/10.1002/esp.4605.
Polyak, V., Hill, C., Asmerom, Y., 2008. Age and evolution of Grand Canyon revealed by U-Pb dating of water-tabletype speleothems. Science 319, 1377–1380. https://doi.org/10.1126/science.1151248.
Regattieri, E., Zanchetta, G., Isola, I., Bajo, P., Perchiazzi, N., Drysdale, R.N., Boschi, C., Hellstrom, J.C., Francke, A., Wagner, B., 2018. A MIS 9/MIS 8 speleothem record of hydrological variability from Macedonia (F.Y.R.O.M.). Glob. Planet. Chang. 162, 39–52. https://doi.org/10.1016/j.gloplacha.2018.01.003.
Richards, D.A., Dorale, J.A., 2003. Uranium-series chronology and environmental applications of speleothems. In: Bourdon, B., Henderson, G.M., Lundstrom, C.C., Turner, S.P. (Eds.), Uranium-series Geochemistry. Mineralogical Society of America, Washington, DC, pp. 407–460. https://doi.org/10.2113/0520407.
Rixhon, G., Braucher, R., Bourlès, D., Siame, L., Bovy, B., Demoulin, A., 2011. Quaternary river incision in NE Ardennes (Belgium) - insights from 10Be/26Al dating of river terraces. Quat. Geochronol. 6, 273–284. https://doi.org/10.1016/j.quageo.2010.11.001.
Rugel, G., Pavetich, S., Akhmadaliev, S., Baez, S.M.E., Scharf, A., Ziegenrücker, R., Merchel, S., 2016. The first four years of the AMS-facility DREAMS: status and developments for more accurate radionuclide data. Nucl. Instrum. Methods Phys. Res., Sect. B 370, 94–100. https://doi.org/10.1016/j.nimb.2016.01.012.
Ruszkiczay-Rüdiger, Z., Balázs, A., Csillag, G., Drijkoningen, G., Fodor, L., 2020. Uplift of the Transdanubian Range, Pannonian Basin: how fast and why? Glob. Planet. Chang. 192, 103263 https://doi.org/10.1016/j.gloplacha.2020.103263.
Ruszkiczay-Rüdiger, Zs., Neuhuber, S., Braucher, R., Lachner, J., Steier, P., Wieser, A., Braun, M., ASTER Team, 2021. Comparison and performance of two cosmogenic nuclide sample preparation procedures of in situ produced 10Be and 26Al. J. Radioanal. Nucl. Chem. 329 (3), 1523–1536. https://doi.org/10.1007/s10967-021-07916-4.
Sasowsky, I.D., Mylroie, J., 2004. Studies of Cave Sediments. Physical and Chemical Records of Paleoclimate. Kluwer Academic/Plenum Publishers, p. 329.
Sauro, F., Fellin, M.G., Columbu, A., Häuselmann, P., Borsato, A., Carbone, C., De Waele, J., 2021. Hints on the Late Miocene evolution of the Tonale-Adamello-Brenta Region (Alps, Italy) based on allochtonous sediments from Raponzolo Cave. Front. Earth Sci. 9, 672119 https://doi.org/10.3389/feart.2021.672119.
Schmid, S.M., Fügenschuh, B., Kounov, A., Matenco, L., Nievergelt, P., Oberhänsli, R., Pleuger, J., Schefer, S., Schuster, R., Tomljenović, B., Ustaszewski, K., van Hinsbergen, D.J.J., 2020. Tectonic units of the Alpine collision zone between Eastern Alps and western Turkey. Gondwana Res. 78, 308–374. https://doi.org/10.1016/j.gr.2019.07.005.
Serpelloni, E., Cavaliere, A., Martelli, L., Pintori, F., Anderlini, L., Borghi, A., Randazzo, D., Bruni, S., Devoti, R., Perfetti, P., Cacciaguerra, S., 2022. Surface velocities and strain-rates in the Euro-Mediterranean Region from massive GPS data processing. Front. Earth Sci. 10, 907897 https://doi.org/10.3389/feart.2022.907897.
Sinopoli, G., Peyron, O., Masi, A., Holtvoeth, J., Francke, A., Wagner, B., Sadori, L., 2019. Pollen-based temperature and precipitation changes in the Ohrid Basin (western Balkans) between 160 and 70 ka. Clim. Past 15, 53–71. https://doi.org/10.5194/cp-15-53-2019.
Steier, P., Martschini, M., Buchriegler, J., Feige, J., Lachner, J., Merchel, S., Milchmayr, L., Priller, A., Rugel, G., Schmidt, E., Wallner, A., Wild, E.M., Golser, R., 2019. Comparison of methods for the detection of 10Be with AMS and a new approach based on a silicon nitride foil stack. Int. J. Mass Spectrom. 444, 116175 https://doi.org/10.1016/j.ijms.2019.116175.
Stone, J.O., 2000. Air pressure and cosmogenic isotope production. J. Geophys. Res. 105, 23753. https://doi.org/10.1029/2000JB900181.
Suc, J.P., Popescu, S.M., Do Couto, D., Clauzon, G., Rubino, J.L., Melinte-Dobrinescu, M. C., Quillevere, F., Brun, J.P., Dumurdzanov, N., Zagorchev, I., Lesi, V., Tomic, D., Sokoutis, D., Meyer, B., Macalet, R., Rifelj, H., 2015. Marine gateway vs. fluvial stream within the Balkans from 6 to 5 Ma. Mar. Pet. Geol. 66, 231–245. https://doi.org/10.1016/j.marpetgeo.2015.01.003.
Temovski, M., 2016. Evolution of Karst in the Lower Part of Crna Reka River Basin. Springer Theses. Springer International Publishing. https://doi.org/10.1007/978-3-319-24547-8.
Temovski, M., Audra, P., Mihevc, A., Spangenberg, J., Polyak, V., McIntosh, W., Bigot, J.-Y., 2013. Hypogenic origin of Provalata Cave, Republic of Macedonia: a distinct case of successive thermal carbonic and sulfuric acid speleogenesis. Int. J. Speleol. 42 (3), 235–246. https://doi.org/10.5038/1827-806X.42.3.7.
Temovski, M., Pruner, P., Hercman, H., Bosák, P., 2016. A cave response to environmental changes in Late Pleistocene: study of Budimirica Cave sediments, Macedonia. Geol. Croat. 69 (3), 307–316. https://doi.org/10.4154/gc.2016.29.
Temovski, M., Túri, M., Futó, I., Braun, M., Molnár, M., Palcsu, L., 2021. Multi-method geochemical characterization of groundwater from a hypogene karst system. Hydrogeol. J. 29, 1129–1152. https://doi.org/10.1007/s10040-020-02293-w.
Vandenberghe, J., 2003. Climate forcing of fluvial system development: an evolution of ideas. Quat. Sci. Rev. 22, 2053–2060. https://doi.org/10.1016/S0277-3791(03)00213-0.
Vermeesch, P., 2007. CosmoCalc: an Excel add-in for cosmogenic nuclide calculations. Geochem. Geophys. Geosyst. 8, Q08003. https://doi.org/10.1029/2006GC001530.
Wagner, B., Vogel, H., Francke, A., Friedrich, T., Donders, T., Lacey, J.H., Leng, M.J., Regattieri, E., Sadori, L., Wilke, T., Zanchetta, G., Albrecht, C., Bertini, A., Combourieu-Nebout, N., Cvetkoska, A., Giaccio, B., Grazhdani, A., Hauffe, T., Holtvoeth, J., Joannin, S., Jovanovska, E., Just, J., Kouli, K., Kousis, I., Koutsodendris, A., Krastel, S., Lagos, M., Leicher, N., Levkov, Z., Lindhorst, K., Masi, A., Melles, M., Mercuri, A.M., Nomade, S., Nowaczyk, N., Panagiotopoulos, K., Peyron, O., Reed, J.M., Sagnotti, L., Sinopoli, G., Stelbrink, B., Sulpizio, R., Timmermann, A., Tofilovska, S., Torri, P., Wagner-Cremer, F., Wonik, T., Zhang, X., 2019. Mediterranean winter rainfall in phase with African monsoons during the past 1.36 million years. Nature 573, 256–260. https://doi.org/10.1038/s41586-019-1529-0.
Zondervan, J.R., Stokes, M., Telfer, M.W., Boulton, S.J., Mather, A.E., Buylaert, J.P., Jain, M., Murray, A.S., Belfoul, M.A., 2022. Constraining a model of punctuated river incision for Quaternary strath terrace formation. Geomorphology 414, 108396. https://doi.org/10.1016/j.geomorph.2022.108396.
Zupan Hajna, N., Bosák, P., Pruner, P., Mihevc, A., Hercman, H., Horáček, I., 2020. Karst sediments in Slovenia: Plio-Quaternary multi-proxy records. Quat. Int. 546, 4–19. https://doi.org/10.1016/j.quaint.2019.11.010.